



ARCHITECTURE & ENGINEERING

Volume 5
Issue 1
March, 2020



By Architects. For Architects.
By Engineers. For Engineers.

Architecture
Civil and Structural Engineering
Mechanics of Materials
Building and Construction
Urban Planning and Development
Transportation Issues in Construction
Geotechnical Engineering and Engineering Geology
Designing, Operation and Service
of Construction Cite Engines

eISSN: 2500-0055

Architecture and Engineering

Volume 5 Issue 1

Editorial Board:

Prof. A. Akaev (Kyrgyzstan)
Prof. Emeritus D. Angelides (Greece)
Prof. S. Bertocci (Italy)
Prof. T. Dadayan (Armenia)
Prof. M. Demosthenous (Cyprus)
T. C. Devezas (Portugal)
Prof. J. Eberhardsteiner (Austria)
V. Edoyan (Armenia)
Prof. G. Esaulov (Russia)
Prof. S. Evtukov (Russia)
Prof. A. Gale (UK)
Prof. G. Galstyan (Armenia)
Prof. Th. Hatzigogos (Greece)
Y. Iwasaki (Japan)
Prof. Jilin Qi (China)
K. Katakalos (Greece)
Prof. N. Kazhar (Poland)
Prof. G. Kipiani (Georgia)
Prof. D. Kubečková (Czech Republic)
Prof. H. I. Ling (USA)
E. Loukogeorgaki (Greece)
Prof. S. Mecca (Italy)
Prof. Menghong Wang (China)
S. A. Mitoulis (UK) Lecturer
Prof. V. Morozov (Russia)
Prof. A. Naniopoulos (Greece)
S. Parrinello (Italy)
Prof. P. Puma (Italy)
Prof. Qi Chengzhi (China)
Prof. J. Rajczyk (Poland)
Prof. M. Rajczyk (Poland)
Prof. Yu. Safaryan (Armenia)
Prof. S. Sementsov (Russia)
A. Sextos (Greece)
E. Shesterov (Russia)
Prof. A. Shkarovskiy (Poland)
Prof. Emeritus T. Tanaka (Japan)
Prof. S. Tepnadze (Georgia)
M. Theofanous (UK) Lecturer
G. Thermou (UK)
I. Wakai (Japan)
Prof. A. Zhusupbekov (Kazakhstan)



Editor in Chief:

Prof. Emeritus G. C. Manos (Greece)

Associate editor:

Marina Deveykis (Russia) Executive Editor



CONTENTS

Civil Engineering

- 3 **Samuel Mahuta Auta, Peter Akwu, Mohammed Saidu**
Effect of Revibration on the Flexural Strength of Concrete Using Mahogany Sawdust Ash as a Partial Replacement for Cement
- 10 **Aleksandr Chernykh, Dmitry Korolkov, Denis Nizhegorodtsev, Tatiana Kazakevich, Shirali Mamedov**
Estimating the Residual Operating Life of Wooden Structures in High Humidity Conditions
- 20 **Vladimir Gryzlov, Alla Kapyushina**
Structural and Mathematical Model of the Thermal Conductivity of Concrete
- 30 **Antonina Judina**
Non-Reagent Methods for the Activation of Concrete Mix Raw Components in the Construction Industry

Geotechnical Engineering and Engineering Geology

- 36 **Vladimir Konyushkov, Van Trong Le**
Side Friction of Sandy and Clay Soils and their Resistance Under the Toe of Deep Bored Piles

Surface Transportation Engineering Technology

- 45 **Stanislav Evtyukov, Egor Golov, Jarosław Rajczyk**
Improving the Accuracy of Stiffness Coefficient Calculation when Estimating the Kinetic Energy Spent on Vehicle Deformation
- 51 **Elena Kurakina, Sergei Evtiukov, Grigory Ginzburg**
Systemic Indicators of Road Infrastructure at Accident Clusters

Civil Engineering

EFFECT OF REVIBRATION ON THE FLEXURAL STRENGTH OF CONCRETE USING MAHOGANY SAWDUST ASH AS A PARTIAL REPLACEMENT FOR CEMENT

Samuel Mahuta Auta¹, Peter Akwu², Mohammed Saidu³

^{1,2,3}Department of Civil Engineering, School of Infrastructures and Process Engineering Technology, Federal University of Technology, Minna, Niger State, Nigeria.

¹Corresponding author: samuel.auta@futminna.edu.ng

Abstract

Introduction: The paper addresses the effect of revibration on the flexural strength of reinforced-concrete beams using mahogany sawdust ash (MSDA) as a partial replacement for ordinary Portland cement (OPC). Beam specimens of sizes 150 mm x 150 mm x 600 mm reinforced with 12 mm diameter steel bars (Y12) and 8 mm diameter steel bars (Y8) as links, were used to cast each of 0%, 5%, 10%, 15% and 20% replacements of cement for SDA. The beams were revibrated after the initial vibration for 20 s at 10-minute successions within one hour. Fifty beams were cast in total and cured for 28 days: 35 revibrated and 15 non-revibrated. **Methods:** Based on the chemical analysis of MSDA, the following major chemical oxides were found in cement: SiO₂ (39.87%), Al₂O₃ (18.05%), Fe₂O₃ (6.92%). Flexural strength tests were carried out for each beam using the three-point load method, and the result shows that the peak flexural strength occurred at 0% followed by 5% replacement at the 20-minute revibration time interval. The revibrated beams show the peak flexural strength of 10.50 N/mm² and 10.00 N/mm² at the 20th minute for 0% and 5% replacements; for the non-revibrated beams, 8 N/mm² and 7 N/mm² were obtained for 0% and 5% replacements, respectively. **Results:** According to the flexural strength test results, revibration has improved the flexural strength of the concrete beams produced, and MSDA as pozzolana is recommended to comfortably replace cement by not more than 5%.

Keywords

Flexural strength, reinforced-concrete beam, revibration, MSDA.

Introduction

The rising cost of traditional building materials (especially, cement) and the devaluation of local currencies of developing nations, makes it difficult for low income earners to own a private house. Those factors have also complicated the construction of civil engineering infrastructure required for national development (Onwuika et al., 2013).

Continuous generation of wastes arising from industrial by-products and agricultural residue create acute environmental problems both in terms of their treatment and disposal. The construction industry has been identified as the one that absorbs the majority of such materials as filler in concrete (Antiohos et al., 2005). If these fillers have pozzolanic properties, they impart technical advantages to the resulting concrete and also enable larger quantities of cement replacement to be achieved (Hossain, 2003). Much less attention is placed on revibration and its importance in concrete production, the process whereby a vibrator is reapplied to concrete at some interval of time after the initial vibration has been carried out (Auta, 2011). A pozzolana is a material which, when combined

with calcium hydroxide, exhibits cementitious properties. Pozzolanas are commonly used as an admixture to Portland cement concrete mixtures to increase the long-term strength and other material properties of Portland cement concrete and in some cases reduce the material cost of concrete. Pozzolanas are primarily vitreous siliceous materials which react with calcium hydroxide to form calcium silicates; other cementitious materials may also be formed depending on the constituents of the pozzolana.

Sawdust ash (SDA) is a waste material from the timber industry. It is produced from logs of timber sawn into planks at sawmills located in virtually all major towns in the country. This process is a daily activity causing heaps of sawdust to be generated after each day. The need to convert this waste product into a useful by-product is the focus of this study (Osey and Jackson, 2012). Some industrial wastes have been studied for use as supplementary cementing materials such as: fly ash (Mathong, 2012); silica fume (Raheem et al., 2012); volcanic ash (Hossain, 2005); rice husk ash (RHA) and corn cob ash (CCA) (Raheem and Adesanya, 2011).

Auta, Abanda and Tsado (2015) and Auta, Amanda, and Sadiku (2015), stated in their findings that flexural strength of RHA concrete increases at the early stage of revibration, the flexural strength of RHA concrete decreases from 30 minutes to 60 minutes of revibration almost for all percentage replacement level of RHA.

Flexural strength of structural elements may be said to be its resistance to bending and is determined either by the ultimate strength of the concrete yield stress f_{ck} or the steel reinforcement f_y . This resistance may then be divided by a proper factor of safety to determine what bending resistance is to be relied upon under working conditions.

According to published findings of researchers, the focus is made on SDA (Auta et al., 2016), which is represented by combinations of different wood species. However, different wood species have different characteristic strengths (Aguwa, 2016). Thus, in this paper, mahogany was determined as a wood species with considerable characteristic strength and hence chosen to produce mahogany sawdust ash (MSDA).

MATERIALS AND EQUIPMENT

Materials

The materials used in this study include:

Fine Aggregate

The fine aggregate (sand) used was clean sharp river sand free of clay, loam, dirt, and any organic or chemical matter, passed through 5 mm British Standard test sieves. It conformed to BS EN 12620 (2013) requirements.

Coarse Aggregate

The coarse aggregate used was gravel free of particles, passed through 10–14mm British Standard test sieves. Quarry gravel was bought from Kpakungu in Minna, Niger State, Nigeria. It conformed to BS EN 12620 (2013) requirements.

Mahogany Sawdust Ash (MSDA)

The sawdust ash was obtained from mahogany wood species sourced from the Dei-Dei timber shed near the Kubwa–Abuja expressway, transported to Minna, sun-dried and then burnt at a controlled temperature of 800°C.

Water

The water used to mix the concrete during this study was free from organic materials and suspended debris. It was obtained from a borehole near the Civil Engineering Laboratory of the Federal University of Technology, Minna. It also conformed to BS EN 1008 (2002) requirements.

Steel Reinforcement

For each specimen, two 12 mm steel bars (Y12) were used as tension bars and two 12 mm steel bars were used as compression bars. 8 mm links were used as well.

Equipment

The equipment used during the study included: a weighing machine, British standard sieves, a head pan, a hand trowel, a tamping rod, buckets, a poker vibrator, a

beam mold (150 mm x 150 mm x 600 mm) and a universal testing machine for the flexural strength test of cured beam specimens.

EXPERIMENTAL PROCEDURES

Procedures

The experimental procedures adopted in this study included the following:

Chemical analysis of MSDA: The chemical analysis of mahogany sawdust ash was conducted at a chemical laboratory where the oxides' composition was determined using X-Ray fluorescent (XRF) tests. This technique was used to discover in-depth information about the chemical composition of MSDA.

Aggregate characterization: The aggregates used for this study were tested for their physical properties such as specific gravity, particle size distribution (sieve analysis) and bulk density.

Preparation of beam specimens: Fifty rectangular beam specimens of 150 mm x 150 mm x 600 mm were produced for the study. Their batching and casting were carried out using the absolute volume method in accordance with BS 1881: part 2 (1970), with a concrete mix ratio of 1:2:4, and a water/cement ratio of 0.5. The main reinforcement used was 12 mm (Y12) diameter tensile steel and the links provided were represented by 8 mm (Y8) bars placed at regular spacing of 125mm c/c. Beam specimens of two types were produced: revibrated and non-revibrated. As for the revibrated beams, 35 beams were produced for percentage replacements (0%, 5%, 10%, 15%, and 20 %) of OPC for MSDA. For each of these percentage replacements, seven beams were cast. The revibration process lasted 20 s at 10-minute successions within one hour. As for the non-revibrated beams, three beam specimens were produced for each percentage replacement to make a sub-total of 15 non-revibrated beams. A poker vibrator was used to compact the concrete mix in the mold for both initial vibration and revibration processes. The beams were de-molded after 24 hours and cured for 28 days. Then, they were tested for flexural strength using a universal testing machine (UTM).

The bending strength test conducted on concrete beams satisfied the requirements of BS 1881-116 (1983) for flexural testing of beams, using the three-point center-point load method as shown in Figure 4. The samples were placed correctly centered, with the longitudinal axis of the beam aligned at a right angle to the supporting and load-applying rollers. This ensured that the top and bottom surfaces of the beam were parallel and the loading was uniform across the width of the beam.

Results and discussion

The laboratory test results included: chemical analysis of MSDA, aggregate characterization, tests on both fresh and hardened concrete. The results are presented in Tables 1, 2, 3, 4, 5, 6 and Figures 1, 2, 3, 4.

Chemical analysis of MSDA: The chemical composition of MSDA used in the study is presented in Table 1. The chemical composition includes: silicon dioxide ($\text{SiO}_2 = 39.873\%$), iron oxide ($\text{Fe}_2\text{O}_3 = 6.924\%$), and aluminium oxide ($\text{Al}_2\text{O}_3 = 18.053\%$), which constitute a total sum of 64.84%, which is slightly below 70% but greater than 50% for a pozzolanic material.

The fly ash, which can be potentially used for concrete, is classified into classes C and F (ASTM C618-19, 2019). The classification is based on the following: if the sum of the three oxides (SiO_2 , Fe_2O_3 and Al_2O_3) above is 70%, the ash is classified as class F, while if the sum 50%, it is classified as class C. In this study, MSDA (a pozzolanic material) falls under class C (ASTM C618-19, 2019).

Table 1. Chemical composition of MSDA

Element	Concentration
Na_2O	1.012
MgO	6.905
Al_2O_3	12.046
SiO_2	49.054
P_2O_5	2.017
SO_3	3.212
Cl	2.412
K_2O	1.224
CaO	11.125
TiO_2	1.562
Cr_2O_3	0.000
Mn_2O_3	0.198
Fe_2O_3	8.935
ZnO	0.209
SrO	0.125

Aggregate characterization: The aggregates and MSDA were tested for specific gravity, particle size distribution, and bulk density.

Particle size analysis for fine, coarse aggregates and MSDA: The results of particle size distribution of MSDA, coarse and fine aggregates used in this study are presented in Table 2, Figures 1 and 2, respectively.

Coarse aggregate particle size analysis: According to Figure 1 below, the grain size corresponding to 60% (D_{60}), 10% (D_{10}) and 30% (D_{30}) is 10.5 mm, 10.1 mm and 10.3 mm, respectively. Therefore, the uniformity coefficient C_u is calculated as equal to 1.04, while the coefficient of curvature C_c is calculated as equal to 1.003. $C_u < 4$ and $1 \leq C_c < 3$ indicates that the gravel is poorly graded in accordance with unified soil classification system (USCS). Therefore, it can be classified as GP.

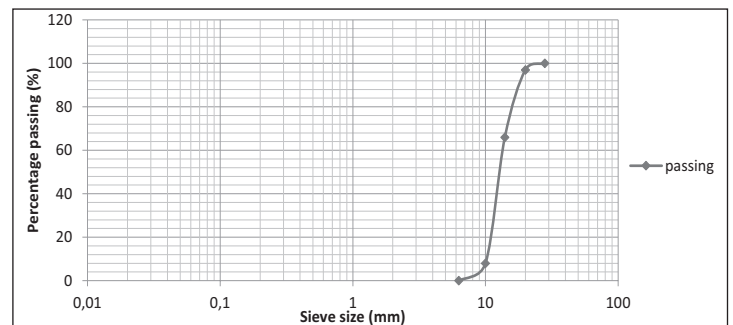


Figure 1. Particle size distribution of coarse aggregate

Fine aggregate particle size analysis: According to Figure 2 below, the grain size corresponding to 60% (D_{60}), 10% (D_{10}) and 30% (D_{30}) is 0.95 mm, 0.35 mm and 0.59 mm, respectively. Therefore, the uniformity coefficient C_u is calculated as equal to 2.70, while the coefficient of curvature C_c is calculated as equal to 1.05. $C_u < 4$ and $1 \leq C_c < 3$ indicates that the sand is poorly graded sand according to the unified soil classification system (USCS). Therefore, it can be classified as SP.

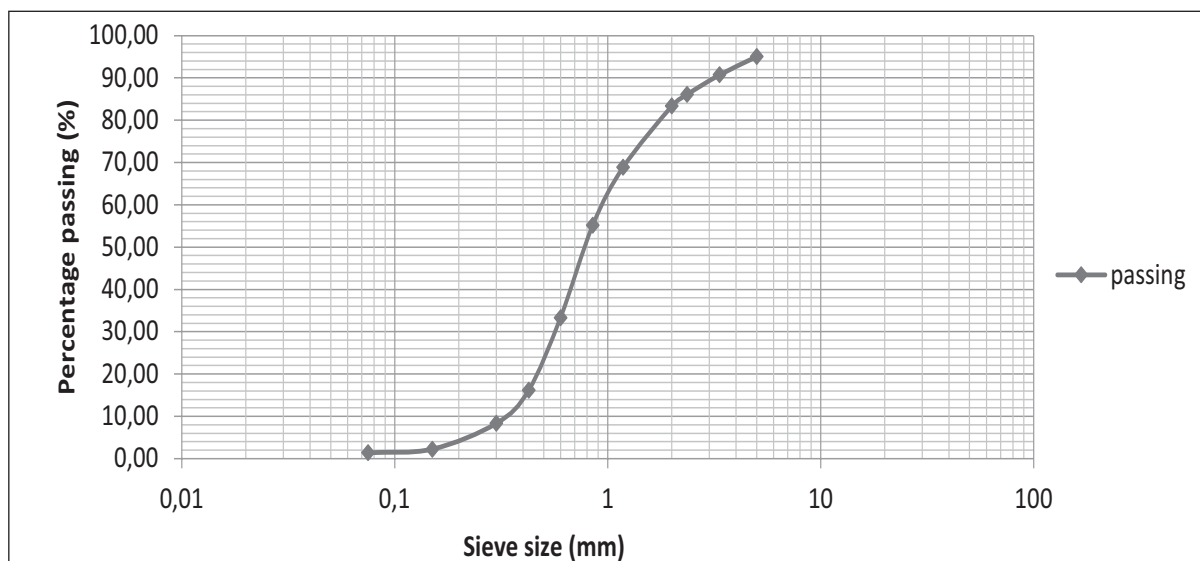


Figure 2. Particle size distribution of fine aggregate

Mahogany sawdust ash particle size analysis

According to Table 2, the MSDA fineness modulus (FM) is obtained as equal to 1.51. The fineness modulus of 1.51 is less than the fineness modulus of 2.1–2.3 for fine

aggregate suggested by American Society for Testing and Materials (ASTM) C 33, hence, MSDA is finer than the fine aggregate.

Table 2. MSDA particle size analysis

Sieve size (mm)	Sample weight retained (g)	Percentage retained (%)	Cumulative percentage retained (%)	Cumulative percentage passing (%)
0.850	0.00	0.00	0.00	0.00
0.600	0.00	0.00	0.00	0.00
0.425	0.00	0.00	0.00	0.00
0.300	22.20	11.10	11.10	88.90
0.150	95.68	47.84	58.94	41.06
0.075	44.39	22.19	81.13	18.87
Pan	36.55	18.27	-	-
Total			151.17	

Specific gravity test of aggregates and MSDA: The specific gravity of MSDA, fine and coarse aggregates is 2.62, 2.65 and 2.63, respectively. Each test was performed thrice with the same sample and the mean specific gravity of each sample was taken. However, the specific gravity of MSDA is less than the specific gravity of cement of 3.15.

difference between the standard cone height and the height of concrete after slump gives the slump value. Table 3 also shows the variation of slump values when cement is partially replaced with MSDA in concrete. The slump value decreases with increasing percentage replacement of OPC with MSDA; this is due to the high demand for water as the ash content increases leading to low workability.

Bulk density test of aggregates and MSDA

The compacted and un-compacted bulk densities of MSDA are 478.91Kg/m³ and 455.88Kg/m³. The compacted and un-compacted bulk densities of coarse aggregate are 1668.82Kg/m³ and 1589.99Kg/m³ and those of fine aggregate are 1534Kg/m³ and 1352Kg/m³.

Compacting factor test: The compacting factor test results are presented in Table 4. The table shows that the compacting factor values decrease as the MSDA content increases. The compacting factor values decreased from 0.92 to 0.84 as the percentage of MSDA replacement increased from 0% to 20% for the revibrated beams. The high demand for water as the MSDA content increased was due to an increase of silica in the mixture. This is different in the case of pozzolana cement concrete as the silica-lime reaction requires more water in addition to water required during hydration of cement (Auta et al., 2016).

Slump test and compacting factor test of fresh MSDA-cement concrete

Slump test: The slump test results for the fresh concrete beams are presented in Table 3 below. The

Table 3. Slump test results for the fresh concrete beams (w/c = 0.5)

No.	Percentage replacement for MSDA (%)	Slump (mm)
1	0	25
2	5	19
3	10	16.5
4	15	14
5	20	No slump

Table 4. Compacting factor test results for the fresh concrete beams

No.	SDA percentage replacement (%)	Compacting factor value
1	0	0.92
2	5	0.88
3	10	0.87
4	15	0.86
5	20	0.85

Effect of revibration on the flexural strength of the revibrated and non-revibrated beams at 28 days curing: Table 5 and 6 show the results of the flexural strength test of each beam specimen for the revibrated beams over time and for the non-revibrated concrete beams, respectively. The mean flexural strength of the control specimen is 9.29 N/mm², which is higher than 5% replacement of MSDA with OPC of 8.93 N/mm² after 28 days curing. The overall mean flexural strength of the specimen reduces from 8.93 N/

mm² to 4.79 N/mm² for 5% to 20% replacement of MSDA with OPC. The peak flexural strength for the revibrated and non-revibrated beams was 10 N/mm² at 20th minutes of revibration (Table 5) and 7.0 N/mm² (Table 6) for 5% replacement, respectively. Table 5 shows that the flexural strength increased significantly from the 0th to 20th minutes of revibration and decreased from the 30th to 60th minutes within the same percentage replacements, indicating that revibration reduced the flexural strength of concrete.

Table 5. Flexural strength of the revibrated concrete beams at 28 days curing

No.	Percentage replacement for MSDA (%)	Flexural strength at each revibration time lag, N/mm ²							Mean flexural strength (N/mm ²)
		0 th min	10 th min	20 th min	30 th min	40 th min	50 th min	60 th min	
1	0	9.5	10.0	10.5	9.5	9.0	8.5	8.0	9.29
2	5	9.0	9.5	10.0	9.5	9.0	8.0	7.5	8.93
3	10	7.5	7.5	8.0	8.5	8.0	7.5	7.0	7.71
4	15	6.5	7.0	7.5	7.0	6.5	6.0	6.0	6.64
5	20	4.0	4.5	5.0	5.5	5.5	4.5	4.5	4.79

Table 6. Flexural strength of the non-revibrated beams at 28 days of curing

No.	Percentage replacement for MSDA (%)	Weight of specimen (kg)	Density of specimen (kg/m ³)	Flexural strength of specimen		Mean flexural strength (N/mm ²)
				bar	(N/mm ²)	
1	0	34.92	2586.67	80	8.0	8.0
		34.24	2536.30	85	8.5	
		35.05	2596.30	75	7.5	
2	5	33.02	2445.93	70	7.0	7.0
		33.05	2448.15	75	7.5	
		33.10	2451.85	65	6.5	
3	10	34.90	2585.19	65	6.5	6.2
		34.85	2581.48	60	6.0	
		34.54	3558.52	60	6.0	
4	15	36.31	2689.63	45	5.5	5.3
		34.65	2566.67	50	5.0	
		33.86	2508.15	55	5.5	
5	20	33.21	2460.00	45	4.5	4.7
		33.87	2508.89	50	5.0	
		32.63	2417.04	45	4.5	

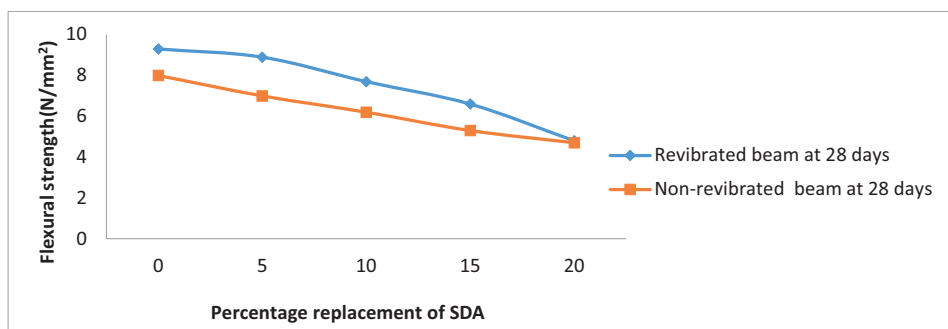


Figure 3. Flexural strength of the revibrated and non-revibrated beams at 28 days curing



Figure 4. Flexural testing of a beam

In Figure 3, the flexural strength values for the revibrated and non-revibrated beams are compared. It clearly indicates that the values for the revibrated beams are higher than those for the non-revibrated ones. This demonstrates the positive effect of revibration on the flexural strength of reinforced MSDA–cement concrete beams. However, the general flexural strength decreases with an increase of MSDA.

Conclusion and recommendations

Conclusion

The effect of revibration on the flexural strength of reinforced-concrete beams using mahogany sawdust ash (MSDA) as a partial replacement for ordinary Portland cement (OPC) is presented. Based on the study, the following conclusions can be drawn:

1. The major constituents of SDA (based on the chemical analysis) include: Al_2O_3 , SiO_2 , and Fe_2O_3 , whose percentage sum of 64.84% is nearly 70% as stipulated by ASTM C 618 (1991) and indicates that MSDA obtained belongs to class F pozzolana.
2. The mean flexural strength values for the revibrated and non-revibrated beams compared clearly indicate that the values for the revibrated beams are higher than those for the non-revibrated demonstrating the positive effect of revibration on the flexural strength.
3. The maximum flexural strength was obtained at the 20th minute of revibration for both 0% and 5% replacements. Others were low both at revibration time intervals and percentage replacements.
4. The compacting factor and flexural strength values decrease as the percentage replacement of SDA increases.

Recommendations

Based on this study, the following recommendations can be made:

The sawdust should be properly assembled, differentiated from other sawdust obtained from other wood species, sun-dried, and burnt; and the chemical analysis of the sawdust should be performed before it is used in concrete production.

The revibration process can always be employed in concrete production to improve the quality of concrete and, when treated with MSDA, 5% replacement of cement should not be exceeded; moreover, revibration beyond 20 minutes is not recommended.

References

- Aguwa, J. I. (2016). *The Nigerian Timber Structures*. Zaira: Ahmadu Bello University Press Limited. 112 p.
- Antiohos, C., Maharaja, S.V., Smart, T.S. (2005). The reaction between rice husk ash and $\text{Ca}(\text{OH})_2$ solution and the nature of its product. *Cement and Concrete Research*, 29 (1), pp. 37–43.
- ASTM International (2019). ASTM C618-19. Standard specification for coal fly ash and raw or calcined natural pozzolan for use in concrete. West Conshohocken: ASTM International. DOI: 10.1520/C0618-19. [online] Available at: <https://www.astm.org/Standards/C618.htm> (accessed on: 12.12.2019).
- Auta, S. M. (2011). Dynamic effect of re-vibration on compressive strength of concrete. *Nigerian Journal of Technological Research*, 6 (2), pp. 13–17.
- Auta, S. M., Abanda, M. A. and Tsado, T. Y. (2015). Experimental study on the flexure strength of a reinforced and re-vibrated RHA concrete beam. In: *Proceedings of 1st International Conference on Green Engineering for Sustainable Development (ICGESD)*, B.U.K., Kano, Nigeria. December,8-10, pp. 54-58.
- Auta, S. M., Amanda, U. and Sadiku, S. (2015). Effect of revibration on the compressive strength. *Nigerian Journal of Engineering and Applied Science (NJEAS)*, 2 (1), pp. 115–121.
- Auta, S. M., Uthman, A., Sadiku, S., Tsado, T. Y. and Shiwua, A. J. (2016). Flexural strength of reinforced revibrated concrete beam with sawdust ash as a partial replacement for cement. *Construction of Unique Buildings and Structures*, 5, pp. 31–45.
- British Standards Institution (1983). *BS 1881: 116. Testing concrete. Method for determination of compressive strength of concrete cubes*. London: British Standards Institution.
- British Standards Institution (2002). *BS EN 1008. Mixing water for concrete*. London: British Standards Institution.
- British Standards Institution (2013). *BS EN 12620. Aggregates for concrete*. London: British Standards Institution.
- Hossain, K. M. A. (2003). Blended cement using volcanic ash and pumice. *Cement and Concrete Research*, 33 (10), pp. 1601–1605. DOI: 10.1016/S0008-8846(03)00127-3.
- Hossain, K. M. A. (2005). Chloride induced corrosion of reinforcement in volcanic ash and pumice based blended concrete. *Cement and Concrete Composites*, 27 (3), pp. 381–390. DOI: 10.1016/j.cemconcomp.2004.02.047.
- Mathong, C. (2012). Sawdust ash (SDA) as partial replacement of cement. *International Journal for Engineering Research and Applications*, 2 (4), pp. 1980–1985.
- Onwuka, D. O., Anyaogu, L., Chijioko C. and Okoye, P. C. (2013). Prediction and optimization of compressive strength of sawdust ash-cement concrete using Scheffe's simplex design. *International Journal of Scientific and Research Publications*, 3 (5), pp. 1–9.
- Osey, D. Y and Jackson, E. N. (2012). Compressive strength and workability of concrete using natural pozzolana as partial replacement of ordinary Portland cement. *Advances in Applied Science Research*, 3 (6), pp. 3658–3662.
- Raheem, A. A. and Adesanya, D. A. (2011). A study of thermal conductivity of corn cob ash blended cement mortar. *The Pacific Journal of Science and Technology*, 12 (2), pp. 106–111.
- Raheem, A. A., Olasunkanmi, B. S. and Folorunso, C. S. (2012). Saw dust ash as partial cement replacement in concrete. *Organization, Technology and Management in Construction. An International Journal*, 4 (2), pp. 474–480. DOI: 10.5592/otmcj.2012.2.3.

ESTIMATING THE RESIDUAL OPERATING LIFE OF WOODEN STRUCTURES IN HIGH HUMIDITY CONDITIONS

Aleksandr Chernykh¹, Dmitry Korolkov², Denis Nizhegorodtsev³, Tatiana Kazakevich⁴, Shirali Mamedov⁵

^{1,2,3,4,5}Saint Petersburg State University of Architecture and Civil Engineering
Vtoraja Krasnoarmeyskaya st., 4, Saint Petersburg, Russia

¹Corresponding author: ag1825831@mail.ru

Abstract

Introduction: The paper addresses the issue of using regression equations to determine the residual operating life of structures made of wood of various species in high humidity conditions. **Purpose of the study:** The study is aimed at deriving general equations for calculation of the ultimate life of wooden structures using univariate regression equations for subsequent calculation of the residual operating life (option 1), or equations for immediate calculation of the residual operating life (option 2). **Methods:** Univariate regression equations are used: linear, logarithmic, second-degree polynomial, power, exponential, natural exponential, and hyperbolic. **Results:** The authors derive general equations for calculation of the ultimate life of wooden structures for subsequent calculation of the residual operating life (option 1), and equations for immediate calculation of the residual operating life (option 2), presenting advantages and disadvantages of both options. They propose an algorithm to process the obtained results in case the calculation is carried out using several equations at once. The authors also present an example of calculating the residual operating life using the second option. **Discussion:** Based on the proposed relationships, it is possible to determine the residual operating life of any wooden structures under any operating conditions.

Keywords

Residual operating life, regression equations, wooden structures, humidity.

Introduction

Wood is one of the oldest materials used in construction. Besides, it is an essential finishing material we cannot do without when building structures, especially residential ones. Wood is still widely used in both exterior and interior finishing. In recent years, the construction of eco-friendly wooden houses has got a second wind.

Wood is both a traditional and modern material. For a while, it gave way to concrete, brick, and other materials. However, engineered wood resumed its rightful place and now it plays an important role in the construction of residential buildings, including high-rise ones (up to 18 stories), public buildings, bridges, sport and industrial facilities. Wood resources recover naturally and relatively quickly. Therefore, the use of wood in construction addresses the issue of sustainable development in society. The share of wooden structures in construction increases rapidly in almost the entire world, and even in those regions that have not significant wood resources. Timber merchants pay much attention to the development of woodworking technologies, improvement of woodworking equipment. New methods of sawing wood of various species, drying and zero-waste processing, joining and gluing pieces make it possible to obtain durable structures of high quality.

Wood has many valuable properties. It is used to manufacture most of the important items, workpieces, and structures for welfare improvement. Wood has a relatively low density (500...600 kg/m³), high strength to weight ratio, low thermal conductivity, and sound insulation characteristics. Among its main advantages, low electrical conductivity and high corrosion resistance can be mentioned. Due to its low electrical conductivity, it can be used as an electrical insulating material for wiring. Such important quality of wood as its eco-friendliness shall be noted as well. Wood is a product of wildlife and it does not emit any harmful substances. Due to its use in construction, it is possible to reduce greenhouse gas emissions into the atmosphere. Obviously, we shall take into account the effect of impregnation compounds intended to increase the protective properties of construction wood. And when such compounds are applied with no procedural violations, the quality of wood will only improve.

Among the disadvantages of wood as a building material, the following can be mentioned: anisotropy of wood; the presence of defects in the material (knots, cracks); the presence of residual deformations in wooden structures; changes in the volume and shape under the action of humidity. Most of the issues related to wooden structures can be compensated for with: a proper design

and suitable wood products; a combination of wood with other fire-resistant, sound-proof or heat-insulating materials; treatment of wooden structures with protective chemical compounds.

All properties of wood mentioned above highlight its significance in our life. Wood remains an essential material used for construction, exterior and interior finishing, creation of various exterior and interior elements, providing comfortable conditions and ensuring design safety of buildings and structures. That is why it is required to estimate the residual operating life of wooden structures.

Residual operating life is the total operating time of an item from the moment of monitoring its technical condition to the moment of reaching the limit state (Rules and Regulations NP-024-2000, State Standard GOST 27.002-2015). It is needed to determine how much longer wooden structures can be in use and what actions can be taken in case the calculated residual operating life is quite short.

Methods

To find a relationship between two variables, regression analysis is used.

The following regression equations are used most often.

1) *Multiple linear regression*:

$$y = \alpha_0 + \alpha_1 \cdot x_1 + \dots + \alpha_n \cdot x_n + \varepsilon \quad (1)$$

Linear regression with one regressor is its special case:

$$y = \alpha_0 + \alpha_1 \cdot x + \varepsilon \quad (2)$$

2) *Polynomial regression*:

$$y = \alpha_0 + \alpha_1 \cdot x + \alpha_2 \cdot x^2 + \dots + \alpha_n \cdot x^n + \varepsilon \quad (3)$$

3) *Power regression*:

$$y = \alpha_0 \cdot x_1^{\alpha_1} \cdot \dots \cdot x_n^{\alpha_n} + \varepsilon \quad (4)$$

4) *Exponential regression*:

$$y = \alpha_0 \cdot \alpha_1^{x_1} \cdot \dots \cdot \alpha_n^{x_n} + \varepsilon \quad (5)$$

5) *Natural exponential regression*:

$$y = e^{(\alpha_0 + \alpha_1 \cdot x_1 + \dots + \alpha_n \cdot x_n)} + \varepsilon \quad (6)$$

6) *Logarithmic regression*:

$$y = \alpha_0 + \alpha_1 \cdot \ln x_1 + \dots + \alpha_n \cdot \ln x_n + \varepsilon \quad (7)$$

7) *Hyperbolic regression*:

$$y = \alpha_0 + \frac{\alpha_1}{x_1} + \dots + \frac{\alpha_n}{x_n} + \varepsilon \quad (8)$$

where

$\alpha_0, \alpha_1, \dots, \alpha_n$ - regression equation parameters;

x_0, x_1, \dots, x_n - independent variables;

ε - the error of approximation;

y - a dependent variable that can be found using the regression equation.

The equations listed above are multivariate. In real practice, univariate regression equations are used to simplify a problem being solved.

Erofeev et al. (2014) studied the strength of wood of various species in high humidity conditions over time using univariate regression equations. Operating time in high humidity conditions was chosen as an independent variable. The error of approximation was neglected since the true value of wood strength is not known (only the average value based on the test results is available).

Following the experimental research, regression equations were obtained for the compressive strength along/ across fibers and bending strength of wood depending on the duration of exposure to high humidity. Here, we present only those equations that have a determination coefficient of more than 0.85 or regression equations with the highest determination coefficient.

Table 1. Regression equations for the compressive strength of wood along fibers depending on the duration of exposure to high humidity

No.	Wood species	Regression equation	Determination coefficient R^2
1	Birch	$y = 86.465 - 2.319x$	0.9893
		$y = 84.624 - 4.9792\ln(x)$	0.9890
		$y = 87.802 - 3.6565x + 0.2675x^2$	0.9999
		$y = 84.659x^{-0.0614}$	0.9864
		$y = 86.621e^{-0.0287x}$	0.9916
2	Redwood	$y = 77.365 - 1.639x$	0.9681
		$y = 75.911 - 3.3266\ln(x)$	0.8648
		$y = 75.703 + 0.0235x - 0.3325x^2$	0.9999
		$y = 75.94x^{-0.0455}$	0.8586
		$y = 77.47e^{-0.0225x}$	0.9647
3	Pine	$y = 52.288 + 14.619x - 2.6925x^2$	0.9122
4	Spruce	$y = 52.927 + 18.195x - 3.5075x^2$	0.9373
5	Ash	$y = 97.563 + 2.8785x - 1.3675x^2$	0.7883
6	Oak	$y = 66.348 + 6.6605x - 1.5175x^2$	0.9880
7	Elm	$y = 63.16 + 2.121x - 0.635x^2$	0.8555
8	Maple	$y = 100.3 - 3.859x$	0.8205
		$y = 90.213 + 6.2285x - 2.0175x^2$	0.9999
9	Linden	$y = 80.9 - 3.287x$	0.9378
		$y = 76.312 + 1.3005x - 0.9175x^2$	0.9962
		$y = 81.382e^{-0.0458x}$	0.9282

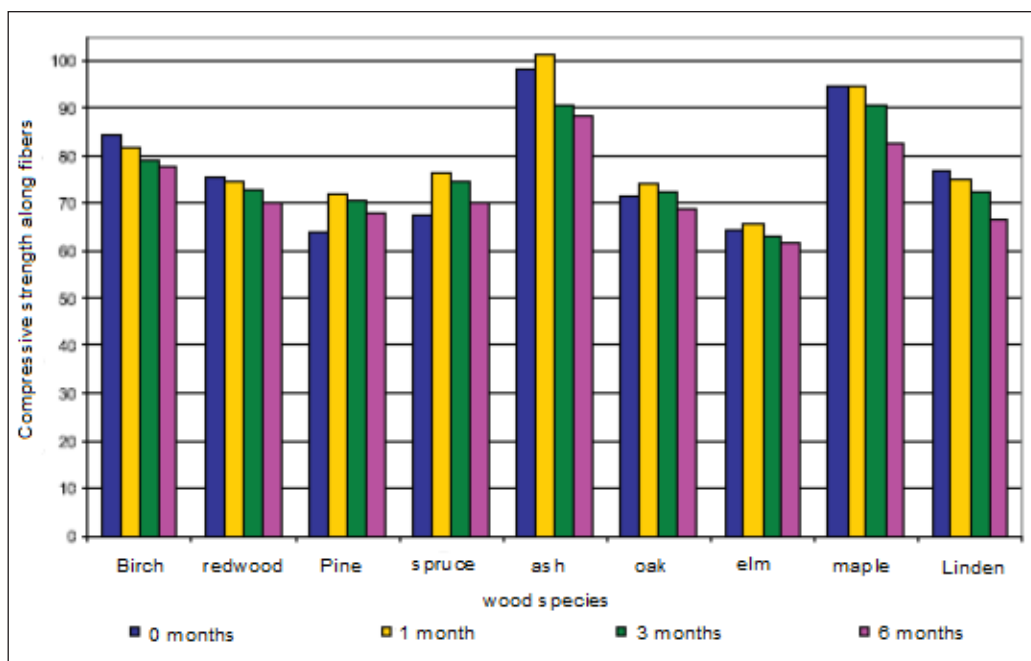


Figure 1. Changes in the strength of different wood species exposed to high humidity, compression along fibers

Table 2. Regression equations for the compressive strength of wood across fibers depending on the duration of exposure to high humidity

No.	Wood species	Regression equation	Determination coefficient R^2
1	Birch	$y = 19.55 - 0.78x$	0.9990
		$y = 18.90 - 1.63\ln(x)$	0.9500
		$y = 19.425 - 0.655x - 0.025x^2$	0.9998
		$y = 18.921x^{-0.0927}$	0.9408
		$y = 19.643e^{-0.0444x}$	0.9974
2	Redwood	$y = 19.565 - 0.562x$	0.8796
		$y = 18.565 + 0.438x - 0.2x^2$	0.9687
		$y = 19.62e^{-0.0312x}$	0.8788
3	Pine	$y = 9.0325 + 2.2665x - 0.4475x^2$	0.7963
4	Spruce	$y = 9.375 + 2.45x - 0.5x^2$	0.9000
5	Ash	$y = 25.063 + 0.0505x - 0.2575x^2$	0.7580
6	Oak	$y = 16.275 + 1.274x - 0.27x^2$	0.9501
7	Elm	$y = 17.663 + 1.1455x - 0.2925x^2$	0.9943
8	Maple	$y = 25.165 - 1.004x$	0.8608
		$y = 22.94 + 1.221x - 0.445x^2$	0.9961
		$y = 25.324e^{-0.0451x}$	0.8507
9	Linden	$y = 19.33 - 1.065x$	0.9140
		$y = 17.668 + 0.5975x - 0.3325x^2$	0.9853
		$y = 19.564e^{-0.0653x}$	0.8984

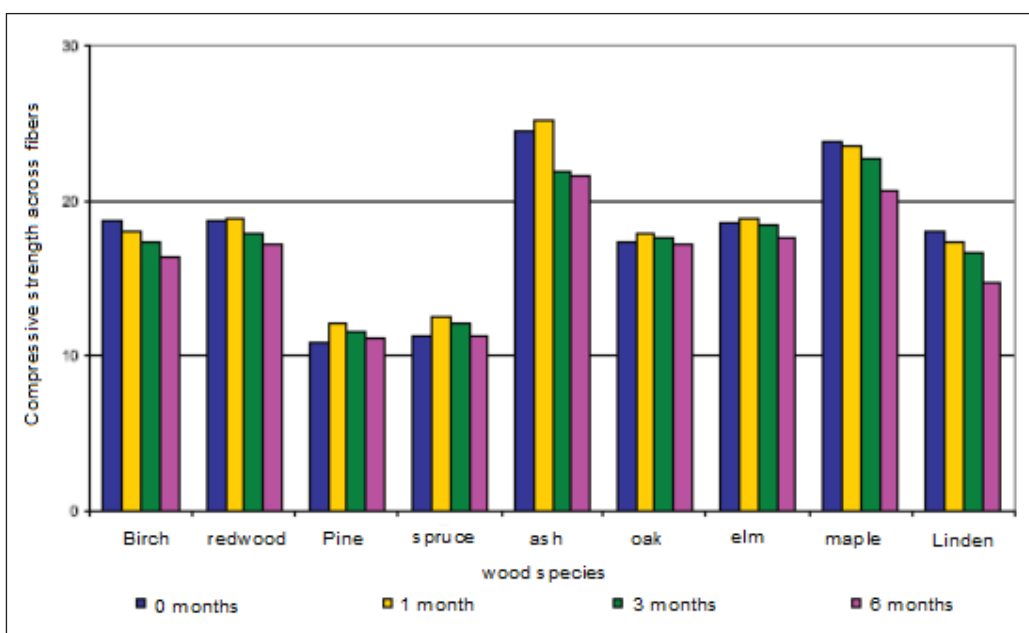


Figure 2. Changes in the strength of different wood species exposed to high humidity, compression across fibers

Table 3. Regression equations for the bending strength of wood depending on the duration of exposure to high humidity

No.	Wood species	Regression equation	Determination coefficient R^2
1	Birch	$y = 754.46 - 37.626x$	0.9424
		$y = 726.46 - 83.154\ln(x)$	0.9981
		$y = 805.18 - 88.351x + 10.145x^2$	0.9972
		$y = 727.24x^{-0.124}$	0.9996
		$y = 758.77e^{-0.0564x}$	0.9531
2	Redwood	$y = 577.65 - 22.032x$	0.9987
		$y = 559.65 - 46.668\ln(x)$	0.9716
		$y = 581.85 - 26.232x + 0.84x^2$	0.9998
		$y = 560.22x^{-0.089}$	0.9654
		$y = 580.01e^{-0.0422x}$	0.9996
3	Pine	$y = 593.45 - 26.61x$	0.9595
		$y = 570.77 - 55.191\ln(x)$	0.8950
		$y = 577.58 - 10.735x - 3.175x^2$	0.9704
		$y = 571.79x^{-0.105}$	0.8792
		$y = 597.4e^{-0.00509x}$	0.9528
4	Spruce	$y = 319.68 + 42.984x - 10.44x^2$	0.9664
5	Ash	$y = 831.78 - 26.856x$	0.9748
		$y = 808.27 - 54.918\ln(x)$	0.8839
		$y = 808.83 - 3.906x - 4.59x^2$	0.9976
		$y = 809.02x^{-0.072}$	0.8736
		$y = 834.58e^{-0.0353x}$	0.9696
6	Oak	$y = 614.81 + 15.007x - 3.7125x^2$	0.7225
7	Elm	$y = 559.57 + 62.595x - 15.525x^2$	1.000
8	Maple	$y = 875.93 - 60.885x$	0.8988
		$y = 761.74 + 53.302x - 22.838x^2$	1.000
		$y = 894.39e^{-0.0868x}$	0.8824
9	Linden	$y = 608.63 - 39.915x$	0.8417
		$y = 515.81 + 52.897x - 18.563x^2$	0.9873

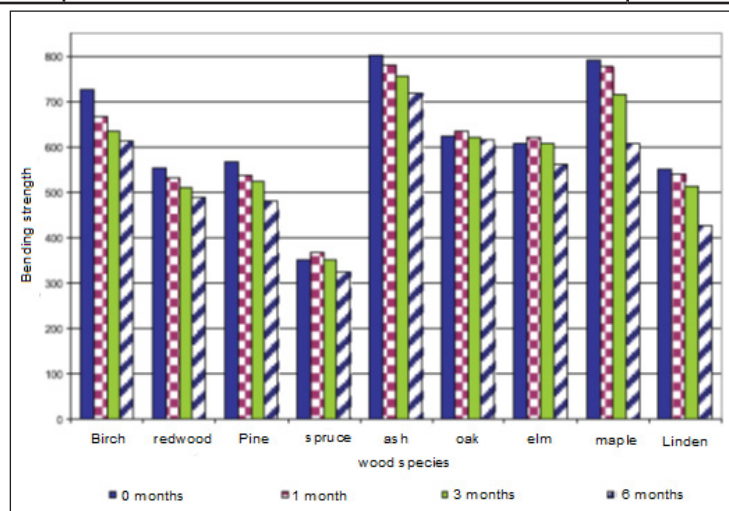


Figure 3. Changes in the bending strength of different wood species exposed to high humidity

As compared with other approaches to the estimation of wooden structures' durability (Chaouch, 2011; Faydi et al., 2017; Hannouz, 2014; Khrulyov, 1981; Köhler, 2006; Lamov, 1999; Perret, 2017), this method is quite interesting as it used regression analysis, which can be applied to any structures and operating conditions.

Results and Discussion

According to the research results, it is possible to estimate the long-term strength of wood using univariate regression equations (with operating time as a variable). Then, the same equations can be used to estimate the residual operating life of wooden structures. It is assumed that operating conditions remain the same during the entire useful life of structures.

This idea can be implemented in two ways. The first one is as follows: if we know the minimum (design) strength of a wooden structure and a regression equation with established parameters, it is possible to determine the ultimate life of such a structure. Subtracting the time, during which it was actually in use, we obtain the residual operating life.

The ultimate life will be as follows.

In case of linear regression:

$$R_{min} = a_1 \cdot t + a_0 \rightarrow t = \frac{R_{min} - a_0}{a_1} \quad (9)$$

In case of logarithmic regression:

$$R_{min} = a_1 \cdot \ln t + a_0 \rightarrow \ln t = \frac{R_{min} - a_0}{a_1} \rightarrow t = \exp \left[\frac{R_{min} - a_0}{a_1} \right] \quad (10)$$

In case of polynomial regression: since second-order equations (parabolic regression) are presented, then the solution will be in the form of a solution to a quadratic equation.

$$R_{min} = a_2 \cdot t^2 + a_1 \cdot t + a_0 \rightarrow a_2 \cdot t^2 + a_1 \cdot t + a_0 - R_{min} = 0 \quad (11)$$

$$t = \frac{-a_1 \pm \sqrt{a_1^2 - 4 \cdot a_2 \cdot (a_0 - R_{min})}}{2 \cdot a_2} \quad (12)$$

The solution has the following constraint: time cannot be a negative value.

In case of power regression:

$$R_{min} = a_0 \cdot t^{a_1} \rightarrow t^{a_1} = \frac{R_{min}}{a_0} \rightarrow t = \sqrt[a_1]{\frac{R_{min}}{a_0}} \quad (13)$$

The constraint will be as follows: $\alpha_1 > 1$.

If α_1 is negative, then we shall divide 1 by t obtained using equation (13).

The solution has the following constraint: time cannot be a negative value.

In case of natural exponential regression: let us present two possible options.

$$R_{min} = a_0 \cdot e^{a_1 \cdot t} \rightarrow e^{a_1 \cdot t} = \frac{R_{min}}{a_0} \rightarrow a_1 \cdot t = \ln \frac{R_{min}}{a_0} \rightarrow t = \frac{1}{a_1} \cdot \ln \frac{R_{min}}{a_0} \quad (14)$$

$$R_{min} = e^{(a_1 \cdot t + a_0)} \rightarrow a_1 \cdot t + a_0 = \ln R_{min} \rightarrow t = \frac{1}{a_1} \cdot (\ln R_{min} - a_0) \quad (15)$$

In case of exponential regression:

$$R_{min} = \alpha_0 \cdot \alpha_1^t \rightarrow \alpha_1^t = \frac{R_{min}}{\alpha_0} \rightarrow t = \log_{\alpha_1} \frac{R_{min}}{\alpha_0} \quad (16)$$

The constraints will be as follows: $\alpha_1 > 0$ и $\alpha_1 \neq 1$.

In case of hyperbolic regression:

$$R_{min} = \alpha_0 + \frac{\alpha_1}{t} \rightarrow \frac{\alpha_1}{t} = R_{min} - \alpha_0 \rightarrow t = \frac{\alpha_1}{R_{min} - \alpha_0} \quad (17)$$

where

α_0 - the initial value of the parameter (strength), MPa;
 α_1 - the rate of the parameter (strength) change, MPa/s;
 α_2 - the rate of the parameter (strength) change acceleration, MPa/s²;

R_{min} - the minimum strength.

Since it is possible to apply several regression equations at once to some wood species, then, in that case, we shall take the arithmetic mean for the operating life. We also can accept the arithmetic mean when establishing the final value if the divergence from the mean does not exceed 10%.

$$t_{mean} = \frac{1}{n} \cdot \sum_{i=1}^n t_i \quad (18)$$

In case of combined stress–strain state, it is required to estimate the ultimate life by several states at once. The least of the obtained values shall be taken as the final value. The least value shall be also chosen if the values are in the range from 10 to 20%.

$$T_{ult} = \min \begin{cases} T_{ult1} \\ \dots \\ T_{ulti} \end{cases} \quad (19)$$

The residual operating life of wooden structures will be as follows:

$$T_{res} = t - t_{serv} \quad (20)$$

where t_{serv} is the actual service life of a structure.

It shall be noted that the equations derived to estimate the ultimate life of wooden structures can be applied to any operating conditions since these equations use abstract parameters a and b .

These equations can be also applied in case of the simultaneous action of several variables.

Then, the residual operating life will be calculated as follows:

$$T_{res} = A \cdot \left[-\frac{1}{B} \cdot t_{serv} + T_{ult} \right] \quad (21)$$

The physical meaning of coefficient *A* is that it reduces the initial (set) residual operating life of building structures due to the immaturity of the manufacturing technology as well as installation and assembly procedures, design errors, etc.

The physical meaning of coefficient *B* is that it reduces the residual operating life of building structures during their use.

Therefore, coefficients *A* and *B* can be considered as safety factors (reduction coefficients).

In the general case, they will take values from 0 to 1.

The disadvantage of this approach is that we need to know the type of regression equation in advance. Such equations are available not for every operating parameter and every wood species.

The second option is as follows: if we know the margin of the load-bearing capacity in wooden structures, it is possible to estimate their residual operating life.

It can be determined in the following way.

In case of linear regression:

$$\Delta R = a_1 \cdot \Delta t + a_0 \rightarrow \Delta t = \frac{\Delta R - a_0}{a_1} \quad (22)$$

In case of logarithmic regression:

$$\begin{aligned} \Delta R &= a_1 \cdot \ln \Delta t + a_0 \rightarrow \ln \Delta t = \\ &= \frac{\Delta R - a_0}{a_1} \rightarrow \Delta t = \exp \left[\frac{\Delta R - a_0}{a_1} \right] \end{aligned} \quad (23)$$

In case of polynomial regression: since second-order equations (parabolic regression) are presented, then the solution will be in the form of a solution to a quadratic equation.

$$\begin{aligned} \Delta R &= a_2 \cdot (\Delta t)^2 + a_1 \cdot \Delta t + a_0 \rightarrow a_2 \cdot (\Delta t)^2 + \\ &+ a_1 \cdot \Delta t + (a_0 - \Delta R) = 0 \end{aligned} \quad (24)$$

$$\Delta t = \frac{-a_1 \pm \sqrt{a_1^2 - 4 \cdot a_2 \cdot (a_0 - \Delta R)}}{2 \cdot a_2} \quad (25)$$

The solution has the following constraint: time cannot be a negative value.

In case of power regression:

$$\Delta R = a_0 \cdot (\Delta t)^{a_1} \rightarrow (\Delta t)^{a_1} = \frac{\Delta R}{a_0} \rightarrow \Delta t = \sqrt[a_1]{\frac{\Delta R}{a_0}} \quad (26)$$

The constraint will be as follows: $\alpha_1 > 1$.

If a_1 is negative, then we shall divide 1 by t obtained using equation (26).

The solution has the following constraint: time cannot be a negative value.

In case of natural exponential regression: let us present two possible options.

$$\begin{aligned} \Delta R &= a_0 \cdot e^{a_1 \cdot \Delta t} \rightarrow e^{a_1 \cdot \Delta t} = \frac{\Delta R}{a_0} \rightarrow a_1 \cdot \Delta t = \\ &= \ln \frac{\Delta R}{a_0} \rightarrow \Delta t = \frac{1}{a_1} \cdot \ln \frac{\Delta R}{a_0} \end{aligned} \quad (27)$$

$$\begin{aligned} \Delta R &= e^{(a_1 \cdot \Delta t + a_0)} \rightarrow a_1 \cdot \Delta t + a_0 = \\ &= \ln \Delta R \rightarrow \Delta t = \frac{1}{a_1} \cdot (\ln \Delta R - a_0) \end{aligned} \quad (28)$$

In case of exponential regression:

$$\Delta R = \alpha_0 \cdot \alpha_1^{\Delta t} \rightarrow \alpha_1^{\Delta t} = \frac{\Delta R}{\alpha_0} \rightarrow \Delta t = \log_{\alpha_1} \frac{\Delta R}{\alpha_0} \quad (29)$$

The constraints will be as follows: $\alpha_1 > 0$ и $\alpha_1 \neq 1$.

In case of hyperbolic regression:

$$\Delta R = \alpha_0 + \frac{\alpha_1}{\Delta t} \rightarrow \frac{\alpha_1}{\Delta t} = \Delta R - \alpha_0 \rightarrow \Delta t = \frac{\alpha_1}{\Delta R - \alpha_0} \quad (30)$$

ΔR - the margin of the load-bearing capacity;

Δt - the residual operating life.

Since it is possible to apply several regression equations at once to some wood species, then, in that case, we shall take the arithmetic mean for the final value of the residual operating life. We also can accept the arithmetic mean when establishing the final value if the divergence from the mean does not exceed 10%.

$$\Delta t_{mean} = \frac{1}{n} \cdot \sum_{i=1}^n \Delta t_i \quad (31)$$

In case of combined stress–strain state, it is required to estimate the residual operating life by several states at once. The least of the obtained values shall be taken as the final value. The least value shall be also chosen if the values are in the range from 10 to 20%.

$$T_{res} = \min \begin{cases} T_{res 1} \\ \dots \\ T_{res i} \end{cases} \quad (32)$$

It is important to note that the residual operating life can be calculated only after it is established that the load-bearing capacity is ensured.

Another disadvantage of this approach is that we need to know the type of regression equation in advance.

Let us present an example of calculation using the second option.

Confirmatory analysis and calculation of the residual operating life for a wooden beam

Table 4. Summary of loads on a wooden beam (distance — 1.5 m)

No.	Load	Standard load, kg/m ²	Coefficient γ^f	Design load, kg/m ²
1	Slab weight	149	1.1	183
2	Live load, 70 kg/m ²	105	1.2	126
	Total (<i>q</i>)	254		309

Operating conditions: heated space, high humidity. Wood species: birch, grade 1.

Normal stress analysis

$h = 20$ cm; $b = 14$ cm; $b_{des} = 14$ cm; $l = 400$ cm; $l_0 = 400$ cm.

$$M = \frac{q \cdot l^2}{8} = \frac{309 \cdot 4^2}{8} = 618 \text{ kg} \cdot \text{m} = 61800 \text{ kg} \cdot \text{cm} \quad (33)$$

According to Clause 7.9 of Regulations SP 64.13330.2017, the following condition shall be fulfilled:

$$M/W_{des} \leq R_b^{des} \quad (34)$$

where R_b^{des} is the design bending strength of wood.

$$R_b^{des} = R_b^A \cdot m_{rup} \cdot m_t \cdot m_m \cdot m_{temp} \cdot m_{u.l.} \quad (35)$$

where $R_b^A = 24 \text{ MPa}$ is the design bending strength for loading mode A (where A is the loading mode No.); $m_{rup} = 0.53$ is the rupture strength coefficient corresponding to loading mode B; $m_t = 1.1$ is the transition coefficient for birch wood; $m_m = 0.9$ is the coefficient taking into account operating conditions 3.1 (moisture conditions); $m_{temp} = 1.0$ is the coefficient taking into account temperature conditions; $m_{u.l.} = 1.0$ is the coefficient taking into account the estimated useful life of a structure.

$$R_b^{des} = 24 \cdot 0.53 \cdot 1.1 \cdot 0.9 \cdot 1 \cdot 1 \cdot 10 = 125.9 \text{ kg/cm}^2 \quad (36)$$

$$W_{des} = \frac{b \cdot h^2}{6} = \frac{14 \cdot 20^2}{6} = 933.33 \text{ cm}^3 \quad (37)$$

$$M/W_{des} = 61800/933.33 = 66.21 \frac{\text{kg}}{\text{cm}^2} < R_b^{des} = 125.9 \text{ kg/cm}^2 \quad (38)$$

The element meets the requirements of Regulations SP 64.13330.2017 regarding the strength under normal stresses.

Shear stress analysis

The element is subject to a transverse force:

$$Q = \frac{q \cdot l}{2} = \frac{309 \cdot 4}{2} = 618 \text{ kg} \quad (39)$$

The following condition shall be fulfilled:

$$\frac{Q \cdot S_{gross}}{I_{gross} \cdot b_{des}} \leq R_{sh}^{des} \quad (40)$$

where S_{gross} and I_{gross} is the static gross moment of inertia

and gross moment of inertia of cross section, R_{sh}^{des} is the design shear resistance of wood along fibers;

$$R_{sh}^{des} = R_{sh}^A \cdot m_{rup} \cdot m_t \cdot m_m \cdot m_{temp} \cdot m_{u.l.} \quad (41)$$

$$R_{sh}^A = 2.7 \text{ MPa}; m_{rup} = 0.53; m_t = 1.3; m_m = 0.9; m_{temp} = 1.0; m_{u.l.} = 1.0.$$

$$R_{sh}^{des} = 2.7 \cdot 0.53 \cdot 1.3 \cdot 0.9 \cdot 1 \cdot 1 \cdot 10 = 16.74 \text{ kg/cm}^2 \quad (42)$$

$$S_{gross} = \frac{b \cdot h^2}{8} = \frac{14 \cdot 20^2}{8} = 700 \text{ cm}^3 \quad (43)$$

$$I_{gross} = \frac{b \cdot h^3}{12} = \frac{14 \cdot 20^3}{12} = 9333.33 \text{ cm}^4 \quad (44)$$

$$\frac{Q \cdot S_{gross}}{I_{gross} \cdot b_{des}} = \frac{618 \cdot 700}{9333.33 \cdot 14} = 3.31 \frac{\text{kg}}{\text{cm}^2} < R_{sh}^{des} = 16.74 \text{ kg/cm}^2 \quad (45)$$

The element meets the requirements of Regulations SP 64.13330.2017 regarding the strength under shear stresses.

Let us determine the residual operating life.

The margin of the load-bearing capacity will be as follows.

For normal stresses:

$$R_{act} = \frac{66.21}{0.53 \cdot 1.1 \cdot 0.9 \cdot 1 \cdot 1 \cdot 10} = 12.62 \text{ MPa} \quad (46)$$

$$\Delta R = 24 - 12.62 = 11.38 \text{ MPa} \quad (47)$$

For shear stresses:

$$R_{act} = \frac{3.31}{0.53 \cdot 1.3 \cdot 0.9 \cdot 1 \cdot 1 \cdot 10} = 0.53 \text{ MPa} \quad (48)$$

$$\Delta R = 2.7 - 0.53 = 2.17 \text{ MPa} \quad (49)$$

Let us assume that the regression equation is known. It will have the following form:

$$\Delta R = 754.46 - 37.626 \cdot \Delta t \quad (50)$$

Then, the residual operating life will be as follows:

$$\Delta t = \frac{11.38 - 754.46}{-37.626} = 19.7 \approx 20 \text{ years} \quad (51)$$

Conclusions

The authors analyzed regression equations for the compressive strength along/across fibers and bending strength of wood of various species over time. For each of them, they derived equations for the estimation of the ultimate life of wooden structures.

They presented two options for the calculation of the residual operating life using regression equations and identified disadvantages of both options.

The authors proposed the following: to take the arithmetic mean for the final value of the ultimate life if the ultimate life is determined using several regression equations at once, or if the divergence from the mean does not exceed 10%. In case of combined stress–strain state or in case the divergence from the mean is in the range from 10 to 20%, the least of the obtained values shall be taken as the final value.

Subtracting the time, during which the structures were actually in use, from the obtained value, we obtain the residual operating life of such structures (first option). In case of the second option, we can obtain the residual operating life right away.

The authors also presented the example of calculating the residual operating life of a wooden beam.

References

Chaouch, M. (2011). *Effet de l'intensité du traitement sur la composition élémentaire et la durabilité du bois traité thermiquement: développement d'un marqueur de prédiction de la résistance aux champignons basidiomycètes*. DSc Thesis in Engineering. Nancy: Université Henri Poincaré – Nancy 1.

Erofeev, V. T., Startsev, O. V., Antoshkin, V. D., Gudozhnikov, S. S., Samolkina, E. G., Boldina, I. V and Makhonkov, A. Y. (2014). Estimation of strength of hardwood in high humidity conditions. *Fundamental Research*, No. 9 (Part 12), pp. 2630–2638.

Faydi, Y., Brancheriau, L., Pot, G. and Collet, R. (2017). Prediction of oak wood mechanical properties based on the statistical exploitation of vibrational response. *BioResources*, 12 (3), pp. 5913–5927. DOI : 10.15376/biores.12.3.5913-5927.

Gosatomnadzor of Russia (2001). Rules and Regulations NP-024-2000. Requirements for justification of the possibility to extend the design service life for nuclear facilities. *Bulletin of Gosatomnadzor of Russia*, 2, pp. 11–17.

Hannouz, S. (2014). *Développement d'indicateurs pour la caractérisation mécanique et la durabilité des bois traités thermiquement*. DSc Thesis in Engineering. Paris: Ecole nationale supérieure d'arts et métiers - ENSAM.

Interstate Council for Standardization, Metrology and Certification (2016). *State Standard GOST 27.002-2015. Dependability in technics. Terms and definitions*. Moscow: Standartinform, 23 p.

Khrulyov, V. M. (1981). *Predicting durability of glue joints in wooden structures*. Moscow: Stroyizdat, 128 p.

Köhler, J. (2006). *Reliability of timber structures*. DSc Thesis in Engineering. Zürich: Eidgenössische Technische Hochschule - ETH Zürich.

Lamov, I. F. (1999). *Improving durability and eco-friendliness of wooden residential buildings used in the climatic conditions of the North*. PhD Thesis in Engineering. Arkhangelsk: Central Research Institute for Wood Machining (TsNIIMOD).

Perret, O. (2017). *Strength and stability of cross-laminated-timber walls at short and long term*. DSc Thesis in Engineering. Champs-sur-Marne: Université Paris-Est.

Ministry of Construction Industry, Housing and Utilities Sector of the Russian Federation (2017). Regulations SP 64.13330.2017. Timber structures. Revised edition of SNiP II-25-80 (Construction Rules and Regulations). Moscow: Standartinform, 97 p.

ОЦЕНКА ОСТАТОЧНОГО РЕСУРСА ДЕРЕВЯННЫХ КОНСТРУКЦИЙ В УСЛОВИЯХ ПОВЫШЕННОЙ ВЛАЖНОСТИ

Александр Григорьевич Черных¹, Дмитрий Игоревич Корольков², Денис Валерьевич Нижегородцев³, Татьяна Николаевна Казакевич⁴, Ширали Махаррамович Мамедов⁵

^{1,2,3,4,5}Санкт-Петербургский государственный архитектурно-строительный университет
2-ая Красноармейская ул., 4, Санкт-Петербург, Россия

¹E-mail: ag1825831@mail.ru

Аннотация

Рассматривается вопрос применения уравнений регрессии для определения остаточного ресурса деревянных конструкций из различных пород древесины в условиях повышенной влажности. **Цель исследования.** Вывод формул расчета предельного срока эксплуатации деревянных конструкций для однофакторных уравнений регрессии в общем виде для последующего расчета остаточного ресурса (вариант №1) либо непосредственно для расчета остаточного ресурса (вариант №2). **Методы.** Используются однофакторные уравнения регрессии: линейное, логарифмическое, полиномиальное второй степени, степенное, экспоненциальное, показательное и гиперболическое. **Результаты.** Выведены уравнения в общем виде для расчета предельного срока службы древесины с последующим расчетом остаточного ресурса (вариант №1), а также уравнения для непосредственно расчета величины остаточного ресурса (вариант №2). Приведены достоинства и недостатки каждого из предложенных вариантов. Предложен алгоритм для обработки полученных результатов, если расчет ведется по нескольким уравнениям сразу. Приведен пример расчета величины остаточного ресурса по второму варианту. **Обсуждение.** С помощью предложенных зависимостей можно рассчитывать величину остаточного ресурса любых деревянных конструкций при любых условиях эксплуатации.

Ключевые слова

Остаточный ресурс, уравнения регрессии, деревянные конструкции, влажность.

STRUCTURAL AND MATHEMATICAL MODEL OF THE THERMAL CONDUCTIVITY OF CONCRETE

Vladimir Gryzlov¹, Alla Kaptyushina²

^{1,2}Cherepovets State University
Lunacharsky Prospect, 5, Cherepovets, Russia

¹Corresponding author: gryvs@mail.ru

Abstract

Introduction: The significance of energy saving in residential construction is associated with the reliable determination of design thermal conductivity characteristics of construction materials. The authors describe a concept of the structural and mathematical modeling of concrete thermal conductivity. The concept is based on methods of the structural approach and generalized conductivity theory. **Purpose of the study:** The study is aimed at developing an adequate structural and mathematical model to determine the thermal conductivity of concrete. **Methods:** The authors used the statistical method as a representation of the statistical homogeneity of a multi-component composite closely related to thermal homogeneity, which is understood as a medium with effective thermal resistance constant in space. **Results:** The authors developed a structural and mathematical model to determine the thermal conductivity of concrete. The model accounts for concrete structural factors existing at the time when the structure formation of concrete is, for the most part, complete. The model also accounts for the thermal and physical properties of concrete components as well as macro- and mesostructural features of concrete. The paper presents calculated data for potential macro- and mesostructural factors, which makes it possible to determine the thermal conductivity of concrete characterized by low thermal conductivity and use the results derived for the approximation of prediction trends related to the thermal properties of such concretes in the operation and adaptation period during the use of building envelopes.

Keywords

Thermal conductivity, structural and technological factor, mathematical model, prediction of thermal and physical properties.

Introduction

The issue of the reliable determination of concrete thermal conductivity is one of the most important in modern construction material engineering. The potential of improving heat-protection efficiency and resource-saving in the manufacturing and operation of building envelopes depends on its successful solution.

The following model of concrete thermal conductivity was suggested in the earlier paper of the author (Gryzlov, 2008):

$$\lambda(t) = \lambda_0 - \Delta\lambda_0(t) e^{-(t-t_0)/\tau} \quad (1)$$

where $\lambda(t)$ is concrete thermal conductivity at fixed time t ; λ_0 is concrete thermal conductivity when the structure formation process is, for the most part, complete (28 days of hardening); $\Delta\lambda_0(t)$ is an increment that occurs as a result of operations during time t ; t_0 is time of intense structure formation; τ is time of thermal conductivity relaxation.

The minus sign before $\lambda_0(t)$ indicates that thermal conductivity adaptation is related to balancing constructive and destructive processes occurring in concrete that, in general, lead to a decrease in internal stress and transition to a stable equilibrium state of exponential nature. Equation (1) can be considered a general equation for the formation and prediction of concrete thermal and physical properties

during the operation of building envelopes. The solution to the prediction problem reduces to the optimization of λ_0 and τ . The λ_0 parameter is a structural and technological aspect of the property, which can be found at the stage of structure selection and formation; the τ value depends not only on the internal parameters of λ but also on the concrete adaptation mode.

According to many researchers (Buzhevich, 1970; Ivanov, 1974; Karamyan, 1976; etc.), the thermal conductivity of concrete is closely related to its density since pores in concrete are filled with air to a large extent. Such an approach is determinative in selecting the design values of thermal conductivity coefficients, and it is captured in regulatory documents (Ministry of Regional Development of Russia, 2012). Table 1 provides empirical equations to determine the thermal conductivity coefficient for inorganic particulate materials, recommended for a wide range of materials, including concrete with a density of $400 \leq \rho \leq 1800 \text{ kg/m}^3$. These equations support the concept of the predominant influence of the material density on its thermal conductivity. However, they also indicate a significant variation of data on the thermal conductivity coefficient at the same density ($\Delta\lambda > 50\%$), which is even more significant in the case of extreme values (Figure 1).

Table 1. Empirical equations to determine the thermal conductivity of concrete

No.	Author	Equation
1	Buzhevich G. A.	$\lambda = 0.38\gamma 10^{-3} - 0.12$
2	Vlasov O. E.	$\lambda = 0.2\gamma + 0.05\gamma^2$
3	Ivanov I. A.	$\lambda = 0.0005\gamma - 0.25$
4	Kaufman B. N.	$\lambda = 0.11\gamma^{1.1} 1.68\gamma + 0.022$
5	Karamyan K. O.	$\lambda = 0.046 + 0.16\gamma^2$
6	Nekrasov V. P.	$\lambda = 1.16 \sqrt{(0.0196 + 0.22\gamma^2)} - 0.16$
7	Spektor B. V.	$\lambda = 0.029 + 2.19 \cdot 10^{-4}\gamma$

λ is the thermal conductivity coefficient; γ is density

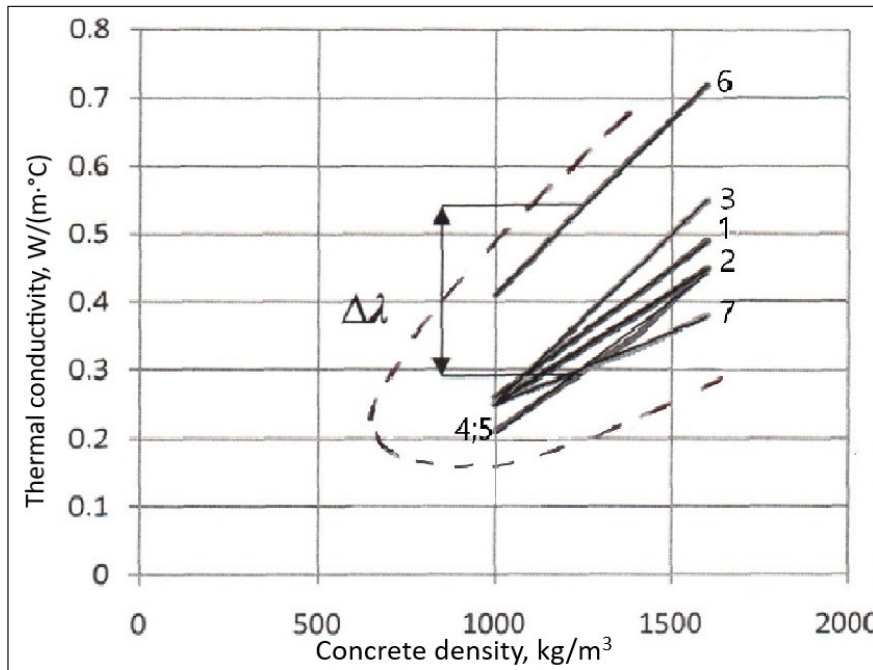


Figure 1 Graphical representation of the equations given in Table 1.

It should be noted that this variation is a consequence of experimental studies conducted by the authors with regard to a certain group of concretes, which confirms that, in the generalized analysis of various types of concrete composites, the structural concept of thermal conductivity exists. The equations given are expressly linear, which indicates a certain bias in the authors' reasoning.

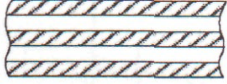
When developing the concept of the influence of concrete porosity on its thermal conductivity, a number of researchers suggested determining thermal conductivity as models of particulates with account for their porosity (Chudnovsky, 1962; Dulnev and Zarechnyuk, 1974;

Krischer, 1934). An analysis of these models has shown that the models by Krischer and Bernshtein are the most appropriate for concrete. To a certain extent, these models interpret the dependence of thermal conductivity on porosity and can be transformed into linear functions of the following type:

$$\lambda_c = \lambda_m - a Pr_{gen} \quad (2)$$

In the case of fixed values of matrix and inclusion thermal conductivity (Table 2), the equations become identical and have the same value of the dimensionless factor a .

Table 2. Models of particulates' thermal conductivity with account for porosity

Author	Model	Equation	* Equation transformed into the following form: $\lambda = f(P)$ at $\lambda_1, \lambda_2 = const$
Krischer O.		$\lambda = \lambda_2 \frac{100}{\frac{\lambda_2}{\lambda_1}(100 - Pr_{gen}) + Pr_{gen}}$	$\lambda_c = \lambda_m - 0.23Pr_{gen}$
		$\lambda = \lambda_1 \frac{100 - Pr_{gen}}{100} + \lambda_2 \frac{Pr_{gen}}{100}$	$\lambda_c = \lambda_m - 0.23Pr_{gen}$
Bernshtein R. S.		$\lambda = \lambda_2 \frac{4Pr_{gen} + \frac{\lambda_1}{\lambda_2}(1 - 2Pr_{gen})}{1 + \frac{\lambda_2}{\lambda_1}}$	$\lambda_c = \lambda_m - 0.23Pr_{gen}$

Note. λ_1, λ_2 are matrix and inclusion thermal conductivity values; Pr_{gen} is general porosity, fractions of volume; *example: $\lambda_1 = 0.54 W / (m \cdot ^\circ C)$; $\lambda_2 = 0.3 W / (m \cdot ^\circ C)$.

The most important thing arising out of the analysis of these models is the confirmation of the statement that, for concretes with continuous matrix structure and minimum porosity, the matrix, i.e. the cement paste (sand-cement mortar), is the main heat conductor.

With regard to the recipe and technological factors as well as macrostructure, mathematical models

describing the dependence of the thermal conductivity coefficient on the inclusion volume are quite interesting (Table 3). While having different mathematical structures, these models, at fixed values, also transform into the linear form, which confirms their qualitative and not quantitative nature.

Table 3. Mathematical models of thermal conductivity with account for the inclusion volume

Author	Equations	*Equation transformed into the following form: $\lambda = f(P)$ at $\lambda_m / \lambda_i = const$
Odelevsky V. I.	$\lambda_c = \lambda_m \left(1 - \frac{P}{\frac{\beta}{\beta-1} - \frac{1-P}{3}} \right)$	$\lambda_c = \lambda_m - 0.22 P$
Dovzhik V. G.	$\lambda_c = \lambda_m \left(\frac{2\lambda_m + \lambda_{inc} - 2P(\lambda_m - \lambda_{inc})}{2\lambda_m + \lambda_{inc} + P(\lambda_m - \lambda_{inc})} \right)$	$\lambda_c = \lambda_m - 0.22 P$
Missenard, A.	$\lambda_c = \lambda_m \left(1 + P \frac{1-\beta}{1 - \sqrt[3]{P} - (1-\beta)} \right)$	$\lambda_c = \lambda_m - 0.22 P$

P is the relative inclusion volume; $\beta = \lambda_m / \lambda_{inc}$; example: $\lambda_m = 0.54 W / (m \cdot ^\circ C)$; $\lambda_{inc} = 0.3 W / (m \cdot ^\circ C)$.

The equations given in Tables 2 and 3, with relevant assumptions, can be transformed into the following form: $\lambda_c = f(\lambda_m, \gamma_c)$, and they have a more information-bearing structure than the equation (Table 1).

$$\lambda_c = f(Pr_{gen}) = \lambda_m - a(1 - \gamma / \gamma_{ctd}) \quad (3)$$

where γ_{ctd} is concrete true density, a is a dimensionless factor.

$$\lambda_c = f(P) = \lambda_m - a(\gamma - 1.23C) / \gamma_{al} \quad (4)$$

where γ_{al} is aggregate density in a lump; C is cement consumption per 1 m³ of concrete.

However, each of the equations, taken separately, does not provide sufficient insight into the influence of the differential distribution of pores, defectiveness of the structure, granulometric, phase and mineral composition of the components on the thermal conductivity of concrete. In this context, the purpose of the study was to:

- **develop a structural and mathematical model to determine the thermal conductivity of concrete that would reflect the influence of its structural factors existing at the time when the structure formation of concrete is, for the most part, complete.**

Methods

Actual multi-component composites consist of particles of no particular form. Therefore, in order to determine the effective thermal conductivity of such media, it is recommended to use the statistical method. This method can be applied to statistically homogeneous media. Visual interpretation of the statistical homogeneity of a medium means that grains of heterogeneous parts shall be sufficiently small as compared to the characteristic dimensions of the body and shall be distributed in a random manner but uniformly in space. Statistical homogeneity is closely related to thermal homogeneity, which is understood as a medium with effective thermal resistance constant in space. When applying the basic concepts of the generalized thermal conductivity theory (Odelevsky, 1951) to a multi-component matrix system, the equation for the calculation of the effective thermal conductivity, provided that the conditions of structural and statistical homogeneity are met, can be transformed into the following form:

$$\lambda_{eff} = \sum \lambda_i v_i^2 + \sum 4\lambda_i \lambda_j v_i v_j / (\lambda_i + \lambda_j) \quad (5)$$

where λ_{eff} is the thermal conductivity coefficient of the system, W/(m·degree); $\lambda_i, \lambda_j, v_i, v_j$ are thermal conductivity coefficients and relative volumes of components, respectively.

This equation is the first approximation to the actual situation. If we present a two-component model of concrete in the form of a layer structure with layers located perpendicular (Figure 2 a) and in parallel (Figure 2 b) to the heat flow (Krischer's model), it is obvious that the first case

will be characterized by the maximum thermal resistance, while the second one will be characterized by the minimum one.

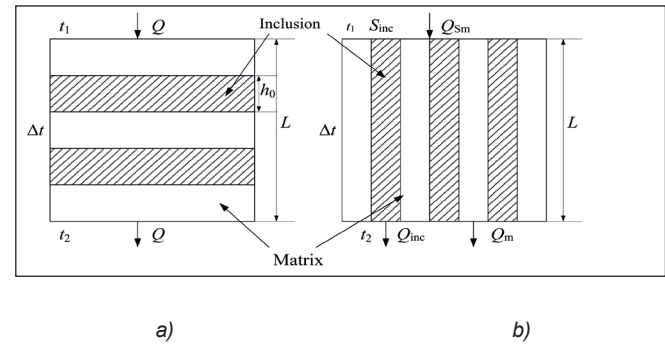


Figure 2. Regarding the calculation of the maximum and minimum thermal resistance of the model:
 a — the layers are perpendicular to the heat flow;
 b — the layers are in parallel to the heat flow

The maximum (R_{max}) and minimum (R_{min}) thermal resistance of this model are described below. Let us assume that λ_m, λ_{inc} are thermal conductivity coefficients with regard to the matrix (binding agent) and inclusion (aggregate); P is the relative inclusion volume, $P_m = 1 - P$ is the matrix volume; $\beta = \lambda_m / \lambda_i$ is the ratio of the thermal conductivity coefficients.

Scheme a. Heat flow Q does not depend on the point on the model surface. In this case, the heat flow is expressed clearly through the difference of temperatures on the opposite surfaces.

$$Q = \frac{\Delta T}{R}$$

$$\text{where } R = \frac{L - h_{inc}}{\lambda_m} + \frac{h_{inc}}{\lambda_{inc}}$$

For a unit layer:

$$R = \left(1 - \frac{h_{inc}}{L}\right) \frac{1}{\lambda_m} + \frac{h_{inc}}{L} \frac{1}{\lambda_{inc}} \quad (6)$$

Since $(h_{inc}/L) = v_{inc}$, equation (6) can be transformed into the following form:

$$R_{max} = [1 + P(\beta - 1)] / \lambda_m \quad (7)$$

which will correspond to the maximum thermal resistance of the model.

Scheme b. Heat flow Q depends on the point on the model surface. In points related to the inclusion:

$$Q_{inc} = \Delta T / (L / \lambda_{inc}) \quad (8)$$

In points related to the matrix:

$$Q_m = \Delta T / (L / \lambda_m) \quad (9)$$

To calculate the average value of Q on the model surface, let us denote the inclusion surface area as S_{inc} ,

and the matrix surface area — as S_m . The total area is equal to: $S = S_{inc} + S_m$.

The average density of the heat flow on the surface S equals to:

$$\dot{Q} = Q_{inc} \frac{S_{inc}}{S} + Q_m \frac{S_m}{S} \tag{10}$$

Let us apply the values of Q_{inc} and Q_m to equation (10). Then, we will obtain the following:

$$Q = \Delta T \left(\frac{S_{inc} \lambda_{inc}}{SL} + \frac{S_m \lambda_m}{SL} \right) \tag{11}$$

Hence, the thermal resistance of the model is as follows:

$$R = \frac{L}{\frac{S_{inc}}{S} \lambda_{inc} + \frac{S_m}{S} \lambda_m}$$

For unit thickness, we will obtain:

$$R = \frac{1}{\frac{S_{inc}}{S} \lambda_{inc} + \frac{S_m}{S} \lambda_m} \tag{12}$$

Taking into account that S_{inc}/S corresponds to P , we will transform equation (12) into the following form:

$$R_{min} = [1 + P(\beta - 1) / (P + (1 - P)\beta)] / \lambda_m \tag{13}$$

which will correspond to the minimum thermal resistance of the model.

By comparing equations (7) and (13), a general structural model of the thermal conductivity of concrete can be found:

$$\lambda_{eff} = \lambda_m / [1 + P(\beta - 1)x] \tag{14}$$

In this equation, x is a dimensionless control factor, which is a product of x' (macrostructural level factor) and x'' (mesostructural level factor). To determine x' , the expression $1 / [P + (1 - P)\beta]$ from equation (13) is used. It should guarantee the minimum error when determining the thermal conductivity of concrete. A nomographic chart of the calculated values of x' is given in Figure 3.

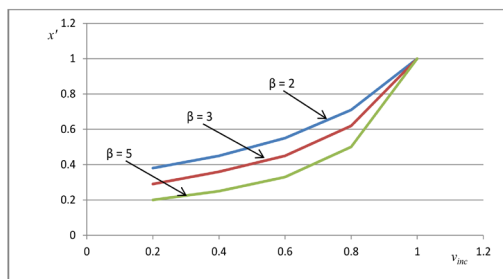


Figure 3. Nomographic chart of the calculated values of x'

In the model under consideration, β is a boundary condition, a peculiar kind of the criterion of sensitivity that

divides concretes into ordinary ones ($\beta < 1$) and those with low thermal conductivity ($\beta > 1$), which is adopted as one of the control factors at the microstructural level.

Results and discussion

The model presented (14) can be considered universal since, through algebraic transformations, a number of known mathematical models of thermal conductivity based on the principles of the generalized conductivity theory (Table 4) are transformed into the form (14), which shows a good approximation of this model with regard to the structural interpretation of the thermal conductivity of concrete. The analysis of the models transformed points at their intermediate value between the values of R_{max} and R_{min} in equations (7) and (13), i.e. each of these models reflects a certain principle of inclusion location between the maximum and minimum values of the thermal resistance indicators and, therefore, the thermal conductivity of concrete. Being structural and mechanical, they do not reflect the influence of physical and chemical processes occurring in the contact area, i.e. they do not take into account the level of the mesostructure.

Table 4. Transformation of known mathematical models of thermal conductivity into the form (14)

Author, source	Dependence type, transformation into the form (14)
Odelevsky V. I.	$\lambda_c = \lambda_m \left[1 - \frac{P}{\frac{\beta}{\beta-1} - \frac{1-P}{3}} \right];$ $\frac{1}{\lambda_c} = \frac{1}{\lambda_m} \left[1 + (\beta-1)P \frac{3}{2(\beta+1-2P(\beta-1))} \right] \tag{14.1}$
Dovzhik V. G.	$\lambda_c = \lambda_m \left[\frac{2\lambda_m + \lambda_{inc} - 2P(\lambda_m - \lambda_{inc})}{2\lambda_m + \lambda_{inc} + 2P(\lambda_m - \lambda_{inc})} \right];$ $\frac{1}{\lambda_c} = \frac{1}{\lambda_m} \left[1 + (\beta-1)P \frac{3}{2\beta+1-2P(\beta-1)} \right] \tag{14.1}$
Missenard, A.	$\lambda_c = \lambda_m \left[1 + P \frac{1-\beta}{1 - \frac{3}{\sqrt{P(1-\beta)}}} \right];$ $\frac{1}{\lambda_m} = \frac{1}{\lambda_m} \left[1 + (\beta-1)P \frac{1}{1 + (\beta-1) \left(\frac{1}{P^{\frac{1}{3}} - P} \right)} \right] \tag{14.2}$
Khlevchuk V. R. Kim L. N.	$\lambda_c = \lambda_m \left[1 + P \frac{1-\beta}{1 - \frac{3}{\sqrt{P(1-\beta)}}} \right];$ $\frac{1}{\lambda_m} = \frac{1}{\lambda_m} \left[1 + (\beta-1)P \frac{1}{1 + (\beta-1) \left(\frac{1}{P^{\frac{1}{3}} - P} \right)} \right] \tag{14.2}$

The assessment of this level was conducted experimentally and made it possible to derive a condition for the assignment of x'' . First of all, it was established that layered models consisting of the cement paste and the aggregate, imitating a contact area, have an integrative indicator of thermal conductivity that is less than the additive one by 10–13% (Kirpichev and Konakov, 1949); at ($\beta > 1$), the following condition is in place: $\lambda_{c.a.} \leq \lambda_{inc} < \lambda_m$ ($\lambda_{c.a.}$ is the thermal conductivity coefficient of the contact area).

To assess the impact of the contact area, we will represent the inclusion as a set n of the fractions of the aggregate. Each fraction consists of cubes with the edge d_i ($d_1 < d_2 < \dots < d_n$). The cubes are oriented in such a way that the heat flow is perpendicular to a surface. The relative share of the i^{th} fraction of the aggregate is a_i , $\sum a_i = 1$. Then, with a known relative aggregate volume P , the values of $P_{c.a.}$ (contact area volume) and P_m (matrix volume) can be determined by the following equations:

$$P_{c.a.} = 2dP(3\sum a_i d_i^2 + 6d\sum a_i d_i + 4d^2) / \sum a_i d_i^3;$$

$$P_m = 1 - P_{c.a.} - P \tag{15}$$

where d is the thickness of the contact layer that depends not on the size of the aggregate particles but on the aggregate technology and material.

Let us consider a parallelepiped with thickness L consisting of the layers of the matrix, contact layer and the aggregate, joined up in series, in a concrete wall. The cumulative thickness values will be as follows:

for the aggregate layers — PL ; for the contact area layers — $2dPL / \sum a_i d_i$; for the matrix layers — $(L - LP - 2dPL) / \sum a_i d_i$.

With the thickness values known, we can find the thermal resistance of the parallelepiped R_p by the following equation:

$$R_p = L [P / \lambda_{inc} + 2dP / \lambda_{c.a.} \sum a_i d_i + (1 - P - 2dP / \sum a_i d_i) / \lambda_m] / S \tag{16}$$

To transform equation (16) into the form corresponding to the general structure of x'' (14), we will introduce following parameters: $D = d/d_i$, i.e. the ratio between the thickness of the contact layer and the size of the aggregate grain, and $\rho = \lambda_m / \lambda_{c.a.}$, i.e. the ratio between the thermal conductivity coefficient of the matrix and the thermal conductivity coefficient of the contact area.

After the transformation, we will obtain:

$$\lambda_{eff} = \lambda_m / [1 + P(\beta - 1)x'(1 + 2D(\rho - 1) / (\beta - 1))] \tag{17}$$

Let us adopt $x'' = 1 + 2D(\rho - 1) / (\beta - 1)$,

By substituting values of x' and x'' in equation (13), we will obtain:

$$\lambda_{eff} = \lambda_m [P + \beta(1 - P)] / [\beta + 2DP(\rho - 1)] \tag{18}$$

where $[P + \beta(1 - P)] / [\beta + 2DP(\rho - 1)]$ can be generally adopted as the structural and technological factor (χ) at the stage of the formation of integrative quality, in this case — the thermal conductivity of concrete.

The results of calculating χ for theoretical and practically possible values of P, β, D, ρ in concretes with low thermal conductivity are given in Table 5.

Table 5. Results of calculating the macro- and mesostructural factor χ in concretes with low thermal conductivity at fixed values of v_{inc}, β, D, ρ

$P\beta$	D	ρ	χ	$P\beta$	D	ρ	χ	$P\beta$	D	ρ	χ			
0.8 2.0	0.2	2.0	0.517	0.75 2.0	0.2	2.0	0.543	0.7 2.0	0.2	2.0	0.614			
		1.5	0.555			1.5	0.581			1.5	0.654			
		1.2	0.581			1.2	0.606			1.2	0.680			
	0.15	2.0	2.0		0.535	0.15	2.0		2.0	0.584	0.15	2.0	2.0	0.633
			1.5		0.566				1.5	0.615			1.5	0.665
			1.2		0.585				1.2	0.635			1.2	0.685
		0.12	2.0		0.548		0.12		2.0	0.596		0.12	2.0	0.645
			1.5		0.572				1.5	0.622			1.5	0.671
			1.2		0.589				1.2	0.638			1.2	0.688
	0.8 1.5	0.2	2.0		0.604	0.75 1.5	0.2		2.0	0.622	0.7 1.5	0.2	2.0	0.646
			1.5		0.662				1.5	0.678			1.5	0.701
			1.2		0.703				1.2	0.718			1.2	0.739
0.15		2.0	2.0	0.632	0.15		2.0	2.0	0.649	0.15		2.0	2.0	0.672
			1.5	0.679				1.5	0.695				1.5	0.716
			1.2	0.710				1.2	0.725				1.2	0.745
		0.12	2.0	0.650			0.12	2.0	0.666			0.12	2.0	0.693
			1.5	0.689				1.5	0.704				1.5	0.726
			1.2	0.715				1.2	0.729				1.2	0.750

continuation of the Table 5.

$P\beta$	D	ρ	χ	$P\beta$	D	ρ	χ	$P\beta$	D	ρ	χ
0.8 1.2	0.2	2.0	0.684	0.75 1.2	0.2	2.0	0.700	0.7 1.2	0.2	2.0	0.716
		1.5	0.764			1.5	0.777			1.5	0.834
		1.2	0.822			1.2	0.833			1.2	0.843
	0.15	2.0	0.722		0.15	2.0	0.726		0.15	2.0	0.752
		1.5	0.788			1.5	0.800			1.5	0.811
		1.2	0.833			1.2	0.843			1.2	0.853
	0.12	2.0	0.747		0.12	2.0	0.760		0.12	2.0	0.774
		1.5	0.802			1.5	0.813			1.5	0.825
		1.2	0.840			1.2	0.849			1.2	0.859

Thus, knowing or assuming the structural and technological characteristics of concretes with low thermal conductivity, using equations (1) and (18), it is possible to approximate the predictive trends of heat-protective properties of these concretes in the operation and adaptation period during the use of building envelopes.

Conclusions

1. The authors developed an adequate structural and mathematical model to determine the thermal conductivity coefficient of concrete. The model accounts for concrete structural factors existing at the time when the structure formation of concrete is, for the most part, complete.

2. This model, albeit a bit complicated, makes it possible to assign the value of the thermal conductivity

coefficient of concrete on a case-by-case basis, taking into account its structural and technological characteristics.

3. It has been confirmed that in concretes with continuous structure, the matrix is the main heat conductor and thermal conductivity factor; the effectiveness of the matrix can be improved or reduced through its modifications or application of the binder with a lower thermal conductivity coefficient.

4. For concretes with low thermal conductivity, the aggregate with the thermal conductivity that is significantly lower than the thermal conductivity of the matrix shall be selected and used, and standard operating procedures, ensuring an increase in the degree of airborne dispersion of the mesostructure and, therefore, an increase in its thickness, shall be applied.

References

- Bernshtein, R. S. (1948). Thermal conductivity of a layer. In: G. G. Knorre (ed.) *Studies of natural fuel combustion processes*. Moscow–Leningrad: Gosenergoizdat, pp. 82–88.
- Buzhevich, G. A. (1970). *Lightweight concrete with porous aggregates*. Moscow: Stroyizdat, 272 p.
- Chudnovsky, A. F. (1962). *Thermal and physical characteristics of disperse materials*. Moscow: Fizmatgiz, 456 p.
- Dovzhik, V. G. (1972). Thermal conductivity of keramzit. *Stroitel'nye materialy*, 3, pp. 21–23.
- Dulnev, G. N. and Zarechnyak, Yu. P. (1974). *Thermal conductivity of mixtures and composite materials*. Leningrad: Energiya, 264 p.
- Gryzlov, V. S. (2008). Universal model of the thermal conductivity of lightweight concrete. *Stroitel'nye Materialy*, 1, pp. 44–46.
- Ivanov, I. A. (1974). *Technology of lightweight concrete with artificial porous aggregates*. Moscow: Stroyizdat, 287 p.
- Itskovich, S. M. (1977). *No-fine concrete*. Moscow: Stroyizdat, 119 p.
- Karamyan, K. O. (1976). *Temperature- and moisture-induced deformations of the building envelope made of lightweight concrete with natural porous aggregates*. Yerevan: Ayastan, 308 p.
- Kaufman, B. N. (1955). *Thermal conductivity of construction materials*. Moscow: State Publishing House of Literature on Construction and Architecture, 160 p.
- Khlevchuk, V. R., Kim, L. N. and Shteinman, B. I. (1983). *Calculation of the thermal conductivity of lightweight concrete depending on structural and technological factors*. *Lightweight concrete house construction*. Moscow: Central Research and Design Institute of Residential Buildings, 121 p.
- Kirpichev, P. V. and Konakov, P. K. (1949). *Mathematical basics of the similarity theory*. Moscow–Leningrad: Publishing House of the USSR Academy of Sciences, 104 p.
- Krischer, O. (1934). Der Einfluß von Feuchtigkeit, Körnung und Temperatur auf die Wärmeleitfähigkeit körniger Stoffe (Die Leitfähigkeit des Erdbodens). *Beihefte zum Gesundheits-Ingenieur*, Series I, No. 33.
- Ministry of Regional Development of Russia (2012). *Regulations SP 50.13330.2012. Thermal performance of the buildings. Revised edition of SNiP 23-02-2003 (Construction Rules and Regulations)*. Moscow: Federal Autonomous Organization "Federal Center for Standardization", 95 p.
- Missenard, A. (1968). *Thermal conductivity of solids, liquids, gases and their compositions*. Moscow: Mir, 464 p.
- Nekrasov, A. A. (1940). Revisiting the dependence of the thermal conductivity coefficient of disperse systems on the external pressure. *Technical Physics*, 10 (2), pp. 168–173.
- Odelevsky, V. I. (1951). Calculation of the generalized conductivity of heterogeneous systems. *Technical Physics*, 21 (6), pp. 667–677.

Spektor, B. V., Svintsitskaya, L. G. and Gutgarts, G. L. (1962). *Thermal and physical characteristics of keramzit perlite concrete*. Kiev: Academy of Construction and Architecture of the Ukrainian Soviet Socialist Republic.

Starostin, F. D. (1935). Calculation of the thermal conductivity of porous solids. *Otopleniye i Ventilyatsiya*, 3, pp. 24–25.

Vlasov, O. E. (1938). *Fundamentals of construction heat engineering*. Moscow: Military and Engineering Academy of the Workers' and Peasants' Red Army, 94 p.

СТРУКТУРНО – МАТЕМАТИЧЕСКАЯ МОДЕЛЬ ТЕПЛОПРОВОДНОСТИ БЕТОНА

Владимир Сергеевич Грызлов¹, Алла Германовна Каптюшина²

^{1,2}Череповецкий государственный университет
Проспект Луначарского, 5, Череповец, Вологодская область, Россия

¹E-mail: gryvs@mail.ru

Аннотация

Актуальность энергосбережения в строительстве жилых зданий непосредственно связана с достоверным определением расчетных теплотехнических характеристик строительных материалов. Изложена концепция структурно – математического моделирования теплопроводности бетона, в основу которой, положены методологии структурного подхода и обобщенной теории проводимости. **Цель исследования.** Разработка адекватной структурно – математической модели по расчету теплопроводности бетона. **Метод.** Использован статистический метод, как интерпретация статистической однородности многокомпонентного композиционного материала, которая тесно связана с термической однородностью, под которой понимается среда с постоянным по пространству эффективным термическим сопротивлением. **Результаты.** Разработана структурно – математическая модель по расчету теплопроводности бетона, учитывающая влияние его структурных факторов, сформированных на момент завершения, в основном, процесса структурообразования. В разработанной модели учитываются теплофизические свойства компонентов бетона, его макро- и мезо-структурные особенности. Приведены расчетные данные практически возможных макро – мезо – структурных факторов, что позволяет определять величину теплопроводности малотеплопроводного бетона и использовать полученные результаты для аппроксимации прогнозных трендов теплозащитных свойств этих бетонов в эксплуатационно – адаптационном периоде работы ограждающих конструкций.

Ключевые слова

Теплопроводность, структурно – технологический фактор, математическая модель, прогноз теплофизических свойств.

NON-REAGENT METHODS FOR THE ACTIVATION OF CONCRETE MIX RAW COMPONENTS IN THE CONSTRUCTION INDUSTRY

Antonina Judina

Saint Petersburg State University of Architecture and Civil Engineering
Vtoraja Krasnoarmeyskaya st., 4, Saint Petersburg, Russia

E-mail: yudinaantonina2017@mail.ru

Abstract

Introduction: The paper presents an analysis of the practice of using non-reagent methods for the activation of raw components, in particular, mixing water for construction (cement, mortar, concrete) mixes. **Purpose of the study:** The study is aimed at the development of effective technologies to reduce the cost and improve the quality of work by activating the raw components of a concrete mix, in particular, mixing water, by non-reagent methods (physico-mechanical effects) at various stages of the process of its preparation. **Methods:** The author conducts theoretical and experimental studies of the effect of mixing water activated by various non-reagent methods on the physico-mechanical and technological properties of concrete. Activated mixing water has a direct impact on hydration and crystallization processes, acceleration of binding agent hardening, etc. During mix preparation, a potential level of concrete quality characteristics is formed, which cannot be raised at the subsequent processing stages. The formation of concrete mix properties starts with mix preparation and continues during its transportation, laying, compaction and hardening. These operations determine concrete quality in building structures and its performance characteristics to a great extent. **Results:** Preparation of a construction (cement, mortar, concrete) mix is an important technological stage in concreting when constructing buildings and structures of cast-in-place concrete and reinforced concrete. In construction practice, various non-reagent methods are used: simple physical (mechanical mixing, heating, deaeration, ionization, etc.), ultrasonic (hydrodynamic processing, use of acoustic field, pulsed electric field processing, etc.), magnetic (constant, variable, pulsed field), and electric (constant, alternating field, high-voltage discharge, electric field of soluble electrodes, etc.). The analysis of various non-reagent methods used to activate mixing water shows that the phenomena occurring in water as a result of its treatment using some of the methods still have not been adequately explained. Nevertheless, the effectiveness of these methods is obvious, but deeper experimental and theoretical studies are needed.

Keywords

Activation, non-reagent methods, mixing water, construction (cement, mortar, concrete) mix, raw components.

Introduction

Thus far, the role and significance of producing and using concrete and reinforced-concrete structures have undergone certain changes. These changes are mainly associated with the transition to cast-in-place as well as cast-in-place and precast construction, which is currently the basic technology for construction of buildings and structures.

Significant expenses for raw materials, supplies and power are the main cost items in manufacturing concrete and reinforced-concrete products and structural units for construction of cast-in-place buildings and structures.

Concrete is the basic construction material, and about 70% of the cement output in Russia is spent for concrete production. To process such amount of resources, efficient and resource-saving technologies involving the use of high-performance machinery and equipment are needed. It is also necessary to find new process solutions for significant concrete quality improvement.

One of the most important concreting operations performed to construct buildings and structures of cast-in-place concrete and reinforced-concrete is concrete mix preparation. In case of low uniformity between concrete quality indicators, cement overconsumption amounts to 10–15%. In case of poor condition of raw components in the concrete mix, cement overconsumption amounts to 5–8%. If it is required to achieve particular concrete characteristics, then, with account for the construction site conditions, cement overconsumption results in significant overconsumption of materials and, therefore, an increase in the cost of construction (Yudina, 2012).

Advances in the study of concrete make it possible to control properties of these materials with regard to resource- and energy-saving as well as improvement of finished products' quality. Studies on the use of non-chemical methods for the activation of construction mix components, and on the design of automated construction mix production lines are very important in construction engineering.

Materials and Methods

Use of various activation methods having physical and mechanical effects on components of the concrete mix (so-called non-reagent methods) is a promising area for the development of the construction (cement, mortar, and concrete) mix preparation technology, and savings in raw materials (Judina and Verstov, 2013).

There is a number of projects related to the activation of concrete mix components (in particular, mixing water) that address the effect of external force fields on mixing water. According to the results of analysis of mixing water activation methods, theoretical interpretations of phenomena occurring both in water during activation (treatment) and at the next stage of mixing with the binding agent have not been studied sufficiently and are often contradictory. Volatility of results regarding concrete strength improvement, hard-to use equipment for water activation, and high power consumption hinder the use of these methods in construction.

Non-reagent methods are the most extensively studied and most often used in construction practice for mixing water treatment. They can be divided into: simple physical (mechanical mixing; heating; deaeration; ionization; etc.), ultrasonic (hydrodynamic processing; use of acoustic field; pulsed electric field processing; etc.), magnetic (constant, variable, pulsed field), and electric (constant, variable field; high-voltage discharge; electric field of soluble electrodes; etc.) methods.

Non-reagent methods of mixing water activation have common features: direct impact on hydration and crystallization processes, acceleration of binding agent hardening, etc. Depending on phenomena occurring in the inter-electrode space, activation methods are classified by activation techniques and according to the specifics of impact created by the external electric field, i.e. its characteristics: frequency, uniformity, etc. Such methods as electrodialysis, electrophoresis, electrocoagulation, dipolophoresis, electric filtering, electroosmosis, electric discharge of low energy, high-voltage pulse discharge, combination of electric actions are given in order of the increasing intensity of the applied electric field (from $E = 0.5\text{--}10\text{ V/cm}$ to 10^4 V/cm) (Biryukov and Spirin, 1983).

Deeper studies on the mechanism of phenomena and processes occurring in water during its activation, and its use to prepare construction mixes to improve physical and mechanical, processing, and performance properties at various stages of concrete mixing, are required (Judina, 2009).

Results and Discussion

Simple physical methods (mechanical mixing; heating; deaeration; ionization; etc.)

Simple physical methods of mixing water activation (simple mechanical mixing, heating under pressure or without pressure, periodic pressure, freezing and thawing, deaeration, ionization, etc.) have been studied and used in construction for a long time.

Application of simple physical actions to mixing water and its subsequent use for construction mix preparation

affect hydration and crystallization processes, accelerate dissolution of calcium silicates in concrete and remove free and bound carbon dioxide. Moreover, such water is capable to reduce the water surface tension and cement paste water requirement as well as accelerate chemical processes upon interaction with the cement minerals (Bertolini et al., 2009; Grushko et al., 1983; Zhang et al., 2006).

Construction mix preparation using pre-heated water (e.g. up to 50°C) ensures acceleration of concrete hardening processes due to greater degree of mixing water and cement activation.

Water deaeration (thermal, vacuum) contributes to the transition of the dissolved air to the disperse state. Adsorption air in the system leads to defects in the contact zone and makes it possible to accelerate dissolution of initial binders and, therefore, increase the crystallization rate of new hydrated formations. Binder dissolution is based on the self-vacuating phenomenon, increases the area of active zones of physical and chemical transformations during cement hydration; acceleration of coagulation processes occurs due to removal of free and bound carbon dioxide. Due to faster structure formation processes, specimen strength gain accelerates by 20% in comparison with that of test specimens made with ordinary water (Grushko et al., 1978).

Mixing water ionization with OH^- and H^+ ions has a positive effect on the mechanism of interaction between the binder and water: hydration duration decreases, structure formation processes accelerate, thus improving concrete strength.

Mixing water processed with electrodialysis differs from ordinary water in higher content of H^+ and OH^- ions and division into acid ($\text{pH} \geq 3$) and alkaline water ($\text{pH} \geq 11$). Studies on the use of ionized mixing water for construction mix preparation show that acid and alkaline water plasticizes the cement paste, plus acid water does that to a greater degree, since it does not affect the initial setting time. However, it increases setting time by half, thus increasing the final setting time as well. Strength and placeability of the mix are also improved (Kalchik and Bulyatova, 1982).

Ultrasound methods (use of acoustic field; hydrodynamic processing; pulsed electric field processing; etc.)

Studies on the effect of acoustic field on water properties gained momentum only recently.

When mixing water is treated with ultrasound, particles with a smaller mass are displaced in relation to particles with a larger mass, which are more inertial, and the relationships between particles change, thus resulting in formation of a particular structure of water.

Water treated with ultrasound and subsequently mixed with the binding agent contributes to formation of numerous micro-cracks in crystals, affecting dissolution of the solid matter. As a result, the active area and the solid phase dissolution rate increase, the dissolved gases are forced out of the surface of solid particles, leading to dissolution

acceleration and more complete hydration of the binding agent. Consequently, additional concrete strength gain is observed at different hardening ages (Zubrilov, 1989).

Magnetic methods (constant, variable, pulsed field)

When mixing water treated with magnetic field is used in construction mix preparation, no stable results are observed with regard to concrete strength improvement. Studies on magnetic field treatment were conducted using water with various impurities, which is why it is impossible to determine what is actually affected: water or its impurities. Therefore, it can be concluded that unstable and incomparable results obtained by different authors are due to different chemical compositions of water.

Chemically pure water is a solution that contains 0.27% of impurities of various isotopic composition and 2–3% of dissolved gases, which apparently were not taken into account. Magnetic field treatment of water represents an issue demanding rigorous theoretical and experimental research. Moreover, along with the parameters (e.g. intensity) of magnetic field and the speed of water flow through such magnetic field, hydrogen ion concentration, gas content in water, etc. should be considered as well.

Due to incorrect selection of the electromagnetic activation mode, absence of treatment effect or even a decrease of strength characteristics of cement stone (concrete) can be observed.

At the same time, according to some findings of studies on electromagnetic treatment of mixing water, concrete strength improvement up to 25% is observed. We can assume that, in case of electromagnetic treatment of mixing water, electrolytic phenomena induced by currents of electromotive forces occur. These phenomena are probably essential for the effect of cement stone strength increase (Fomichev et al., 2015).

Electric methods (constant, variable field; high-voltage discharge; electric field of soluble electrodes)

The use of electric methods for treatment of water and water systems in various areas is most efficient if the type of electric field action and parameters of electric field are chosen correctly. Parameters of electric field differ in the action of uniform constant electric field *E-Const* (rather sufficiently studied in water purification and associated with electrophoresis, polarization interaction and electrocoagulation phenomena); uniform variable electric field *E²-Const* (less efficient and mainly associated with polarization coagulation); uniform constant and non-uniform variable field (associated with the dielectrophoresis and dipolephoresis effect); electric discharge characterized by such three physical and chemical phenomena as pre-breakdown, breakdown and post-discharge stages.

As for electric actions, treatment of liquids with uniform constant electric field is the most studied. Electrochemical processes of electrode material dissolution and metal hydroxide formation represent the main factor affecting dispersion of low field intensities. Water treated with external electric field of soluble electrodes made of various metals differs from ordinary water in the increased

content of H^+ and OH^- ions and increased concentration of multivalent electrode metal hydroxide ions (Svetlitsky, 1980).

Treatment of mixing water with electric field of soluble electrodes affects coagulation, structure- and hydrate formation, as well as formation of the condensation and crystallization structure of cement stone. Such structure is formed due to direct chemical interaction of particles (with development of a rigid space structure). Parameters of mixing water activation using electric field affect coagulation of particles in the dispersed phase. Applying this method when preparing a concrete mix, it is possible to rule out the use of chemicals and additives, automate both the mixing water activation (treatment) process and the entire process of concrete mix preparation (Yudina, 2000; Yudina, 2019).

The author conducted experimental studies on the effect of mixing water treated by electric field of soluble electrodes. The results showed that the use of such water affects the improvement of the physico-mechanical and technological properties of both cement and concrete mixes.

Mixing water activated using a high-voltage electric discharge contributes to acceleration of cement minerals' hardening.

The effect of a constant electric discharge manifests to the fullest extent in the pre-breakdown phase. The shock wave initiates cavitation, electromagnetic pulsed field and thermal radiation. These processes affect mixing water the most if the discharge is periodic and near critical. In this case, specific energy is generated in the discharge channel at the highest speed (Romashchenko, 1995).

There are many other methods of water treatment as well: radiation treatment based on the action of X-ray beams, light-hydraulic effect (laser beam action on water). Some researchers conducted experiments in autoclave water treatment at 200–500°C and elevated pressures as well as in "pulsars" (devices creating alternating pressures in water). However, these are searching methods, and their applied significance can be reviewed in further studies.

Conclusions

The analysis of various non-reagent methods of mixing water activation (physical and mechanical actions) shows that, when some methods of mixing water activation are used, theoretical phenomena occurring in water after its treatment are poorly explained and proved, and in many cases, they do not ensure stable efficiency improvement.

Such methods as magnetic or ultrasound treatment, use of an electric discharge, etc. require much power and hard-to-use equipment for water treatment, which significantly increases mix production cycle time and the cost of the finished product.

It should also be noted that activation methods with the use of electric field of soluble electrodes usually do not require changing the entire concrete mix preparation process, and after mixing with the use of such water, it becomes possible to control mix hardening.

With a slight increase in the cost of concrete mix production, processing and performance properties of concrete improve significantly.

The studies on mixing water treatment with uniform constant electric field, aimed to analyze the influence of the field on concrete characteristics, were carried out by the author in laboratory and industrial conditions.

It is obvious that non-reagent methods are efficient. However, deeper experimental and theoretical studies are required. Significant contradictions in the explanations of the processes occurring both in water and during its mixing with the binder hinder wide application of these rational methods in practice.

References

- Bertolini, L., Coppola, L., Gastaldi, M. and Redaelli, E. (2009). Electroosmotic transport in porous construction materials and dehumidification of masonry. *Construction and Building Materials*, 23 (1), pp. 254–263.
- Biryukov, V. A. and Spirin, Y. A. (1983). Influence of integrated physical and chemical mixing water treatment on the phase composition of cement stone. In: *Implementation of the Regional Integrated R&D Target Program "Concrete"*, Kharkov, pp. 49–65.
- Fomichev, V. T., Erofeev, V. T., Emelyanov, D. V., Matvievskiy, A. A. and Mitina, E. A. (2015). The role of the products of anodic processes during electromagnetic water activation. *Fundamental Research*, Issue 2, Part 6, pp. 1194–1197.
- Grushko, I. M., Mank, V. V., Belova, L. A. et al. (1983). On the mechanism of the intensifying action of water treatment on structure formation process in concrete. *Zhurnal Prikladnoi Khimii*, 56, pp. 813–814.
- Grushko, I. M., Mikhailov, A. F. and Pilipenko, V. V. (1978). On self-vacuuming of concrete mixes tempered with deaerated water. *Izvestiya Vuzov. Stroitelstvo i Arkhitektura*, pp. 136–147.
- Judina, A. F. (2009). Activation of concrete mix components using non-reagency techniques. *Building Tender*, 43, pp. 76–77.
- Judina, A. and Verstov, V. (2013). On efficient use of electric treatment methods in the technology of concrete work. *World Applied Sciences Journal 23 (Problems of Architecture and Construction)*, pp. 9–12. DOI: 10.5829/idosi.wasj.2013.23.pac. 90003.
- Kalchik, G. S. and Bulyatova, E. N. (1982). *Use of ionized water in manufacturing of precast reinforced-concrete products. Theory, production and use of artificial conglomerates*. Vladimir, 206 p.
- Romashchenko, N. M. (1995). *Concrete properties and its production using a high-voltage electric discharge. PhD Thesis in Engineering*. Saint Petersburg: Emperor Alexander I St. Petersburg State Transport University.
- Svetlitsky, A. S. (1980). *Clarification of water in an electric field with the aid of soluble electrodes. Author's summary of PhD Thesis in Engineering*. Leningrad: Leningrad Institute of Engineering and Construction.
- Yudina, A. F. (2000). *Resource-saving concreting technology based on the use of electrically treated mixing water. DSc Thesis in Engineering*. Saint Petersburg: Saint Petersburg State University of Architecture and Civil Engineering.
- Yudina, A. F. (2012). Advantages of monolithic building, and some problems of its perfection. *Bulletin of Civil Engineers*, 1, pp. 154–156.
- Yudina, A. F. (2019). Enhancing technological processes in building construction and reconstruction by means of new technologies. *Asian Journal of Civil Engineering*, 20 (5), pp. 727–732. DOI: 10.1007/s42107-019-001139-9.
- Zhang, D.-J., Xu, S.-L. and Sun, J. (2006). Experimental study on electric properties of CFRM and CFRC. *Jianzhu Cailiao Xuebao/ Journal of Building Materials*, Vol. 9, pp. 347–352.
- Zubrilov, S. P. (1989). *Physical activation of solutions*. Leningrad: Publishing House of the Academy of Sciences of the USSR, 185 p.

НЕРЕАГЕНТНЫЕ МЕТОДЫ АКТИВАЦИИ СЫРЬЕВЫХ КОМПОНЕНТОВ БЕТОННОЙ СМЕСИ В СТРОИТЕЛЬСТВЕ

Антонина Федоровна Юдина

Санкт-Петербургский государственный архитектурно-строительный университет
2-ая Красноармейская ул., 4, Санкт-Петербург, Россия

E-mail: yudinaantonina2017@mail.ru

Аннотация

Проведён анализ практики использования нереагентных методов активации сырьевых компонентов, в частности воды затворения строительной смеси (цементной, растворной и бетонной) в строительном производстве. **Цель исследования.** Разработка эффективных технологий, позволяющих снизить стоимость и повысить качество работ путем активация сырьевых компонентов бетонной смеси, в частности воды затворения, нереагентными методами (физико-механическими воздействиями) на различных этапах технологического процесса ее приготовления. **Методы.** Теоретические и экспериментальные исследования влияния воды затворения активированной различными нереагентными методами на физико-механические и технологические свойства бетона. Активированная вода затворения оказывает непосредственное воздействие на процессы гидратации и кристаллизации, ускорение процессов твердения вяжущего и т. п. В процессе приготовления формируется потенциальный уровень характеристик качества бетона, который не может быть повышен на последующих технологических переделах. Формирование свойств бетонной смеси начинается с ее приготовления и продолжается при транспортировании, укладке, уплотнении и твердении. Эти операции во многом определяют качество бетона в конструкциях зданий и его эксплуатационные характеристики. **Результаты.** Приготовление строительной смеси (цементной, растворной и бетонной) - важный технологический этап в комплексе бетонных работ при возведении зданий и сооружений из монолитного бетона и железобетона. В практике строительного производства нереагентные методы используются различные методы - простые физические (механическое перемешивание, нагревание, деаэрация, ионизация и др.), ультразвуковые (гидродинамическая обработка, акустическое поле импульсная обработка и др.), магнитные (постоянное, переменное, импульсное поле), электрические (постоянное, переменное поле, высоковольтный электрический разряд, электрическое поле растворимых электродов и др.). Проведенный анализ различных методов активации воды затворения нереагентными методами показал, что до сих пор при использовании некоторых методов недостаточно полно объяснены явления, происходящие в воде в результате ее обработки. Тем не менее эффективность этих методов очевидна, но нужны более глубокие экспериментальные и теоретические исследования.

Ключевые слова

Активация, нереагентные методы, вода затворения, строительная смесь (цементная, растворная и бетонная), сырьевые компоненты.

Geotechnical Engineering and Engineering Geology

SIDE FRICTION OF SANDY AND CLAY SOILS AND THEIR RESISTANCE UNDER THE TOE OF DEEP BORED PILES

Vladimir Konyushkov¹, Van Trong Le²

^{1,2}Saint Petersburg State University of Architecture and Civil Engineering
Vtoraja Krasnoarmeyskaya st., 4, Saint Petersburg, Russia

¹Corresponding author: v.konyushkov@yandex.ru

Abstract

Introduction: Saint Petersburg is characterized by complex engineering and geological conditions due to the presence of a significant mass (with a thickness of 20...30 m or more) of highly deformable soils with deformation moduli of 5...10 MPa. Besides, due to long-term geological processes that took place in the territory of Saint Petersburg thousands of years ago, these soils are extremely unevenly distributed in depth and area of occurrence. However, according to modern requirements for city development, deeper underground structures and higher buildings are needed. In terms of geotechnical solutions, it is possible to meet these requirements by using deep piles. **Purpose of the study:** The authors of the paper made an approximate brief classification of the geological conditions of Saint Petersburg based on the genesis, depth of occurrence, and physical and mechanical properties, and developed a method for more accurate calculations of the bearing capacity of deep bored piles. **Methods:** In the course of the study, the authors performed statistical processing of 600 values of the bearing capacity of bored piles, calculated according to the requirements of standards and determined by the results of field tests. In addition, they performed a non-linear extrapolation of side friction and resistance values (for soils with a depth of up to 100 m). **Results:** The paper presents the assessment of the bearing capacity of bored piles depending on their depth in glacial moraine and pre-quadernary vendian deposits. Using the nonlinear extrapolation, the authors calculated the side friction and resistance under the toe of bored piles for further design of pile foundations with deep bored piles (at a depth of up to 100 m). **Discussion:** According to statistical studies, the actual bearing capacity of bored piles is significantly higher than the design one calculated according to the requirements of corresponding standards (by 1.6...2.6 times). This is due to the fact that soils with significantly differing strength and deformation characteristics are located along the side and under the toe of bored piles. The stronger the soil where the most part of the pile is located, the more the bearing capacity error is (towards underestimation). The paper presents studies confirming this statement.

Keywords

Glacial moraine and pre-quadernary vendian deposits, side friction, resistance under the pile toe, bearing capacity of bored piles at a depth of up to 100 m.

Introduction

The authors of the paper conducted a large-scale analysis of archival materials related to engineering and geological surveys performed by GUP "Trest GR11" (State Unitary Enterprise "Geodetic and Engineering Survey Trust") and ZAO "LenTISIZ" (Closed Joint-Stock Company "Leningrad Engineering and Construction Survey Trust") in Saint Petersburg over the past 50 years. Following the analysis results, an approximate classification of soils was

made based on their genesis, depth of occurrence, and physical and mechanical properties. In general, in terms of genesis, soils in Saint Petersburg can be divided into four main sedimentary complexes (Dashko et al., 2011; Filippov and Spiridonov, 2009; Shashkin, 2014):

0. Technogenic deposits (tg_{IV}) — located in the upper part of the soil mass, starting from the level of the grade elevation of the ground. They are characterized

by extremely uneven stratification in depth and area of occurrence. Due to heterogeneous configuration, their strength and deformation properties differ significantly. As a rule, during surveys, these soils are not assigned any characteristics, which is why they are usually not used as load-bearing soils and bases under the foundations of buildings and structures. Their thickness usually does not exceed 1.5...5 m (but it may be higher in some areas).

1. River and marine deposits (al_{IV} , ml_{IV}) — located under technogenic deposits. As a rule, they are represented by water-saturated silty sands and sandy loams, sometimes clay loam. Silty sands are usually characterized by medium strength and deformability (in contrast to lower values of sandy loams and clay loams' characteristics). These soils are located under the foundation bottom of most historical buildings in Saint Petersburg (with a construction and operation period of more than 100 years). Their thickness is usually insignificant and amounts to 1...5 m (however, it can be higher). It should be noted that, according to modern design requirements, these soils cannot be used as the bearing layer or the base for foundations of permanent facilities in every instance. This is due to their insignificant thickness and presence of highly deformable lake-glacial deposits underlying the base of river and marine deposits.

2. Lake-glacial deposits (lg_{IV}) — can be located directly under technogenic deposits or under river or marine deposits (although they may interstratify with those). They are mainly represented by sandy loams and clay loams. Their strength and deformation characteristics are extremely unfavorable: these soils are highly deformable, poorly permeable, overmoistened, thixotropic and creeping. Long-term geological processes of their formation and historical processes of Saint Petersburg development and construction are responsible for the fact that lake-glacial deposits represent the underlying layers of bearing soils under most of the foundations of buildings and structures constructed on a natural base (from the foundation of Saint Petersburg in 1703 to the present time). It is a consequence of the long-term development of differential settlements in the foundations of historical and modern buildings constructed on a natural base or on short piles (placed in such soils).

3. Glacial moraine deposits (g_{III}) — represented mainly by sandy loams and clay loams; located, as a rule, under lake-glacial deposits. These soils are characterized by medium strength (as compared with overlying soils). However, characteristics of glacial deposits vary significantly due to different genesis, structure, composition, depth, thickness, and extension. Glacial deposits can be classified as mainly medium-deformable but, in some cases, they can also be highly deformable for the reasons outlined above. The majority of buildings and structures on pile foundations (both constructed and under construction) in Saint Petersburg have glacial moraine deposits as bearing layers under the pile toe.

4. Pre-Quaternary Vendian clays (vkt_2) — the most durable and reliable layer, which is represented by solid and semi-solid clays. The top of this layer is extremely uneven in depth (usually at significant depths from 20 m and deeper). However, when penetrated, the top of this layer is usually homogeneous in terms of its properties: engineering and geological elements below have strength and deformability not less than those of overlying elements, and sometimes these values even increase in depth. We can state that the foundations based on undisturbed pre-Quaternary Vendian clays will have a significant bearing capacity and low deformations. As already mentioned above, the main disadvantage of this complex is the uneven depth of the top and the significant depth of occurrence in some areas of Saint Petersburg (up to 60...80 m or more).

Figures 1 and 2 below show schematic maps of Saint Petersburg indicating the depth of the top of glacial moraine and pre-Quaternary Vendian deposits. Table 1 shows the approximate values of the physical and mechanical characteristics of the main geological deposits in Saint Petersburg depending on their genesis (highly deformable, medium- deformable and poorly deformable soils are highlighted in different colors).

Subject, tasks, and methods

The subject of the study is the bearing capacity of deep bored piles subjected to a vertical compressive load. To perform the study, the authors developed a brief classification of genetic complexes of Saint Petersburg soils (Figures 1, 2, Table 1). Then, they set and solved the following **tasks**:

- classified results of 600 field tests of bored piles, performed by OOO "PKTI Fundament-Test" for the period from 2000 to 2020, and performed their statistical processing;
- constructed comparative diagrams for the bearing capacity of bored piles, calculated according to the requirements of standards and obtained as a result of field tests;
- determined the side friction of sandy and clay soils depending on the soil properties and pile depth of up to 100 m;
- determined the resistance of sandy and clay soils under the pile toe depending on the soil properties and pile depth of up to 100 m.

As the main research **methods**, the authors used statistical processing of 600 values of the pile bearing capacity, calculated according to the requirements of standards and obtained as a result of field tests (using the least square method). Besides, they performed a non-linear extrapolation of friction and resistance values to a depth of 100 m, depending on the physical properties of soils (based on the corresponding tables in Regulations SP 24.13330 "Pile foundations", limiting the pile length to 40 m).

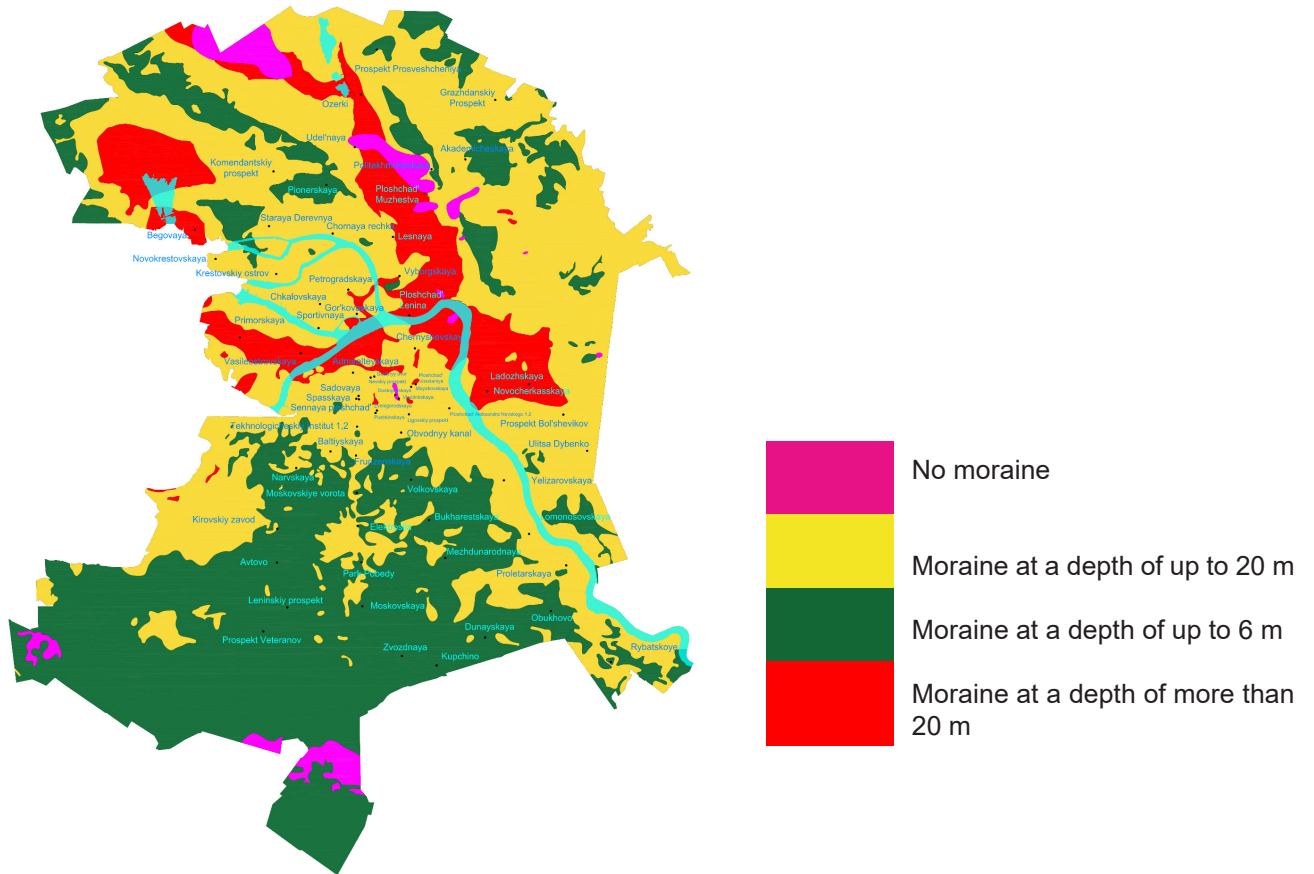


Figure 1. Schematic map of Saint Petersburg with color representation of the depth of the top of glacial Moraine deposits

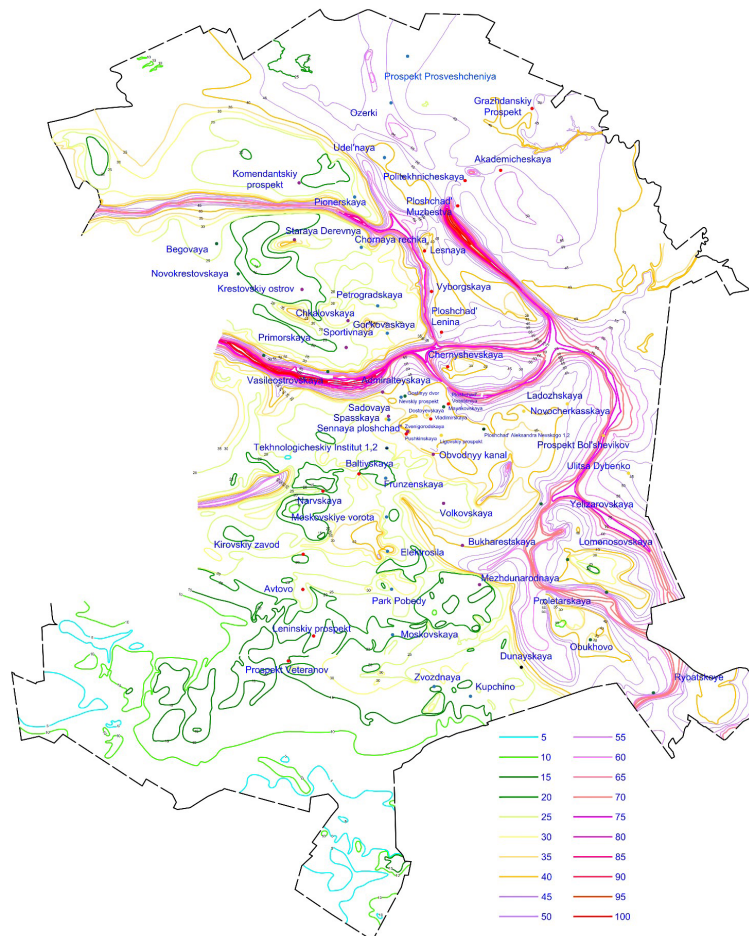


Figure 2. Schematic map of Saint Petersburg with isolines for the depth of the top of pre-quaternary vendian deposits, m

Table 1. Approximate values of physical and mechanical characteristics of soils in Saint Petersburg depending on their genesis (red color indicates highly deformable soils, yellow color indicates medium-deformable soils, and green color indicates poorly deformable soils)

Parameter	Designation, unit	Name of soil genesis			
		1. Properties of river and marine deposits (al_{IV}, ml_{IV})	2. Properties of lake-glacial deposits (lg_{IV})	3. Properties of glacial moraine sandy loams and clay loams (g_{III})	4. Properties of pre-quaternary vendian clays (vkt_2)
Specific weight	$\gamma, \text{kN/m}^3$	17...20	17...20	18...20	20...22
Moisture	$W, \%$	50...30	50...30	30...20	20...10
Void ratio	$e, \text{unit fraction}$	more than 1.0...0.6	more than 1.0...0.6	0.8...0.5	0.5...0.3
Liquidity index	$I_L, -$	more than 1.0...0.75 (for clay soils)	more than 1.0...0.75 (for clay soils)	0.75...0.25	less than 0.25
Specific cohesion	c, kPa	1...20 (for sand)	5...20	20...50	50...100 and higher
Internal friction angle	$\varphi, ^\circ$	20...30 (for sand)	5...20	15...30	15...30
Deformation modulus	E, MPa	5...15	5...15	15...40	20...100 and higher

Results and discussion

The bearing capacity of a bored pile mainly depends on two components: side friction forces and soil resistance under the pile toe (Gotman et al., 2017; Ilyichev and Mangushev, 2016; Konyushkov et al., 2019; Mangushev et al., 2010, 2014; Osokin et al., 2019; Shulyatyev, 2016; Shulyatyev et al., 2017; Ter-Martirosyan, 2009; Ter-Martirosian et al., 2017; Ter-Martirosyan et al., 2015):

$$F_d = f(\sum f_i; R_i) \quad (1)$$

With an increase in the pile depth (Figure 3), the side friction and the resistance under the pile toe can be classified into three characteristic cases as shown in expressions (2) and (3):

$$\sum f_1 < \sum f_2 < \sum f_3 \quad (2)$$

$$R_1 < R_2 < R_3 \quad (3)$$

Figure 3 shows a provisional classification for the bearing capacity of bored piles (three main schemes) depending on the pile depth in weak soils, moraine and Vendian deposits.

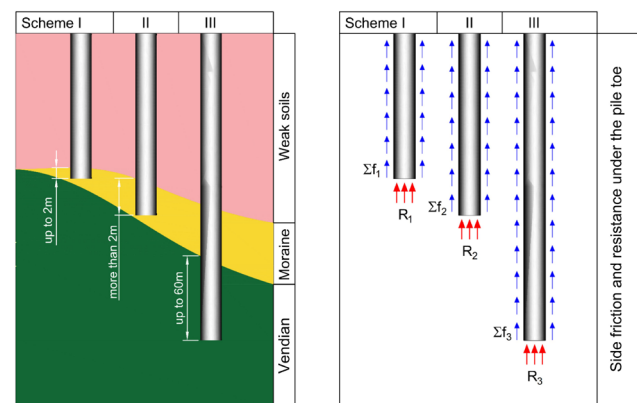


Figure 3. Provisional classification for the bearing capacity of bored piles (three main schemes) depending on the pile depth in weak soils, moraine and vendian deposits

We analyzed the extensive results of the field tests of bored piles, performed in Saint Petersburg by OOO “PKTI Fundament-Test” during 2000–2020. In total, approximately 600 tests were processed. After that, we calculated the bearing capacity of bored piles using the method suggested by Regulations SP 24.13330 “Pile

foundations”. Then, we constructed comparative diagrams for the bearing capacity of piles based on the field tests and the bearing capacity of piles calculated according to the requirements of standards. Figures 4, 5, 6 show results of statistical processing of bearing capacity ratios obtained by the least square method. All comparative diagrams clearly show that, depending on the location of a pile in the ground (schemes I, II, III in Figure 3), the actual bearing capacity of a pile determined based on the results of the field tests, increases by 1.6...2.6 times. This fact indicates that the greater the pile depth is (especially if it is a solid ground, e.g. pre-quaternary Vendian clay according to scheme III), the more the actual bearing capacity of the pile differs from that calculated according

to the requirements of standards. We expanded the well-known table of soil frictions and resistances depending on the physical properties of soils from Regulations SP 24.13330 “Pile foundations”. This table is characterized by a pile depth limit to 40 m. Using a nonlinear extrapolation, we constructed graphs for the distribution of side friction and soil resistance under the pile toe up to a depth of 100 m. Tables 2, 3 and Figures 7, 8 show results of such nonlinear extrapolation of friction and resistance values. Taking into account the fact that pile foundations for high-rise buildings currently require a depth of more than 40 m (e.g. piles for the Lakhta Center have a depth of 85 m from the grade elevation of the ground), these tables and graphs can be very useful for designers and builders.

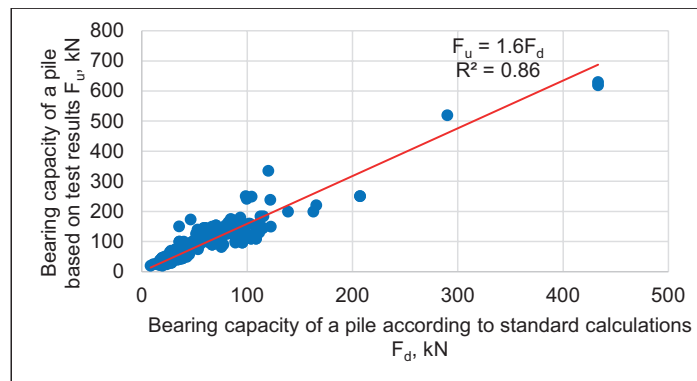


Figure 4. Comparative diagram for the bearing capacity of bored piles based on the results of field tests and bearing capacity of bored piles calculated according to standards (scheme I)

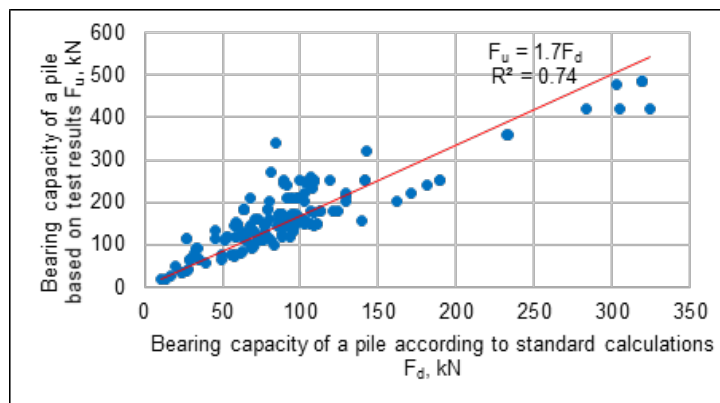


Figure 5. Comparative diagram for the bearing capacity of bored piles based on the results of field tests and bearing capacity of bored piles calculated according to standards (scheme II)

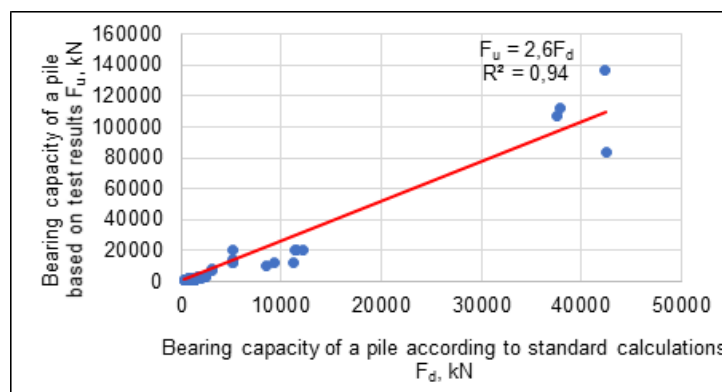


Figure 6. Comparative diagram for the bearing capacity of bored piles based on the results of field tests and bearing capacity of bored piles calculated according to standards (scheme III)

Table 2. Side friction of sandy and clay soils

Design side friction f , kPa					
Medium density sands	coarse and medium	Clay soils with liquidity index I_L	0.2	$f = 34.716z^{0.2861}$	$R^2 = 0.9936$
	fine		0.3	$f = 24.349z^{0.2902}$	$R^2 = 0.9898$
	silty		0.4	$f = 16.917z^{0.3058}$	$R^2 = 0.9820$
	-		0.5	$f = 14.259z^{0.2644}$	$R^2 = 0.9477$
	-		0.6	$f = 10.503z^{0.2261}$	$R^2 = 0.8386$
	-		0.7	$f = 5.6088z^{0.2518}$	$R^2 = 0.8369$
	-		0.8	$f = 5.1753z^{0.1694}$	$R^2 = 0.6849$
	-		0.9	$f = 4.148z^{0.2027}$	$R^2 = 0.6752$
	-		1.0	$f = 3.241z^{0.2372}$	$R^2 = 0.6844$

Notes:

1. z is the average depth of the soil layer, m.
2. f is the design side friction, kPa.
3. When calculating the design side friction f , the soil layers shall be divided into homogeneous layers with a thickness not exceeding 2 m.
4. The design side friction values f for dense sands shall be increased by 30% compared with the values given in the table.
5. The design friction values for sandy loams and clay loams with a void ratio $e < 0.5$ and clays with a void ratio $e < 0.6$ shall be increased by 15% compared with the values given in the table at any values of the liquidity index.

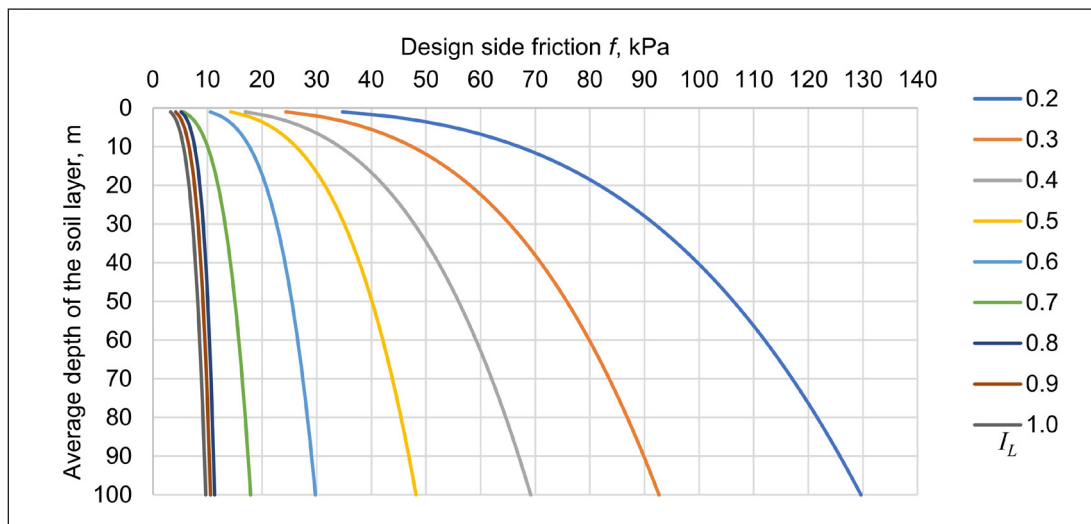


Figure 7. Graph for the distribution of side friction forces up to a depth of 100 m

Table 3. Resistance of sandy and clay soils under the toe of bored piles

Design resistance under the toe of bored piles R , kPa					
Medium density sands	Gravelly	Clay soils with liquidity index I_L	0.0	$R = 0,7287z^2 + 67,372z + 636,88$	$R^2 = 0,9998$
	Coarse		0.1	$R = 0,4504z^2 + 69,632z + 500,81$	$R^2 = 0,9996$
	-		0.2	$R = 0,2499z^2 + 67,026z + 408,23$	$R^2 = 0,9984$
	Medium		0.3	$R = 0,0403z^2 + 65,742z + 302,9$	$R^2 = 0,9998$
	Fine		0.4	$R = -0,2019z^2 + 66,531z + 171,75$	$R^2 = 0,9991$
	Silty		0.5	$R = -0,0861z^2 + 59,195z + 110,29$	$R^2 = 0,9985$
	-		0.6	$R = -0,2276z^2 + 51,595z + 99,61$	$R^2 = 0,9985$

Notes:

1. z is the depth of the pile toe, m
2. R is the design resistance under the toe of a bored pile, kPa
3. for intermediate values of the liquidity index I_L for clay soils, the R values in the table are determined by interpolation.

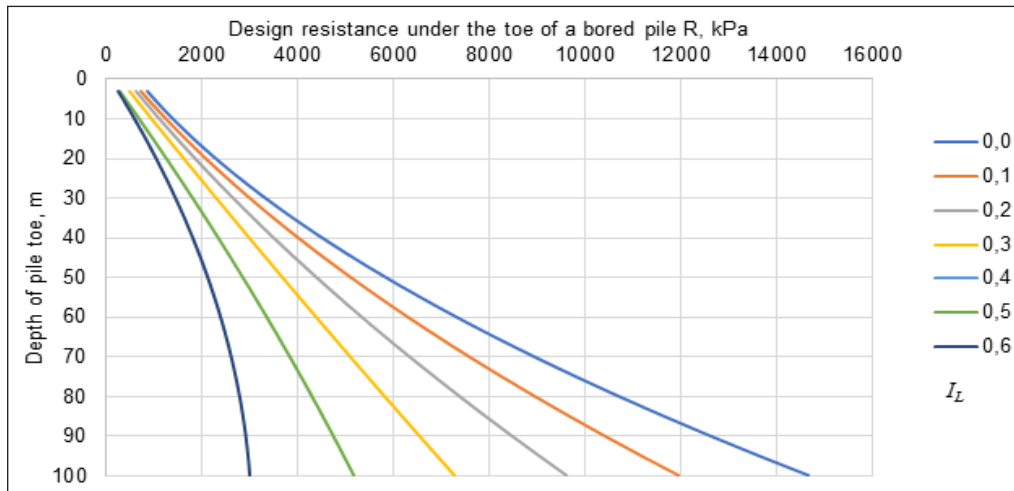


Figure 8. Graph for the distribution of soil resistance under the toe of a bored pile up to a depth of 100 m

Conclusions

Based on the archival materials of geological surveys performed by GUP "Trest GR11" (State Unitary Enterprise "Geodetic and Engineering Survey Trust") and ZAO "LenTISIZ" (Closed Joint-Stock Company "Leningrad Engineering and Construction Survey Trust"), the authors developed the schematic maps for the depth of the top of glacial moraine deposits and pre-Quaternary Vendian clays, which are typically load-bearing soils of pile foundations. At the stage of preliminary design of foundations, it is possible to use these maps and determine the length of piles based on the location of a construction site in Saint Petersburg.

Based on the statistical processing of the results of 600 field tests of bored piles, performed by OOO "PKTI Fundament-Test", it was found that the actual bearing capacity of bored piles significantly exceeds the design one, calculated according to the requirements of corresponding standards (by 1.6...2.6 times). With an increase in the depth of piles in stronger soils, the actual bearing capacity and the design one can differ by 2.6 times.

For more accurate calculations of the bearing capacity of deep bored piles, the authors performed the nonlinear extrapolation of side friction and resistance (under the toe of piles up to a depth of 100 m) values depending on the physical characteristics of soils where the piles are located. The results of the nonlinear extrapolation are summarized in tables and graphs, the use of which will make it possible to perform more accurate calculations of the bearing capacity of deep bored piles.

Acknowledgments

The authors express their gratitude to General Director of ZAO "LenTISIZ" Nikolay N. Oleynik for providing archival materials related to geological surveys performed in Saint Petersburg and General Director of OOO "PKTI Fundament-Test" Grigory V. Levintov for materials related to field tests of piles.

Funding

The study was performed without any funding outside of the author's own funds and on the personal initiative of the authors.

References

- Dashko, R. E., Aleksandrova, O. Yu., Kotyukov, P. V. and Shidlovskaya, A. V. (2011). Specifics of engineering and geological conditions in Saint Petersburg. *Urban Development and Geotechnical Construction*, 1, pp. 1–47.
- Filippov, N. B. and Spiridonov, M. A. (eds.) (2009). *Geological Atlas of Saint Petersburg*. Saint Petersburg: Komilfo, 57 p.
- Gotman, N. Z., Alekhin, V. S. and Sergeev, F. V. (2017). Determination of bearing capacity of piles in the group. *PNRPU Bulletin. Construction and Architecture*, 8 (3), pp. 13–21. DOI: 10.15593/2224-9826/2017.3.02.
- Ilyichev, V. A. and Mangushev, R. A. (eds.) (2016). *Geotechnical engineer's reference book. Bases, foundations, and underground constructions*. 2nd edition. Moscow: ASV Publishing House, 1040 p.
- Konyushkov, V. V., Kondratieva, L. N., Kirillov, V. M. and Le Van Trong (2019). Accelerated methods for determining the bearing capacity of drill piles. *Bulletin of Civil Engineers*, 3, pp. 63–71. DOI: 10.23968/1999-5571-2019-16-3-63-71.
- Mangushev, R. A., Ershov, A. V. and Osokin, A. I. (2010). *Modern pile technologies*. 2nd edition. Moscow: ASV Publishing House, 240 p.
- Mangushev, R. A., Konyushkov, V. V. and D'yakonov, I. P. (2014). Analysis of practical application of screw-in cast piles. *Soil Mechanics and Foundation Engineering*, 51 (5), pp. 227–233.
- Mangushev, R. A., Osokin, A. I. and Sotnikov, S. N. (2018). *Geotechnics of Saint Petersburg. Experience in construction on weak soils*. Moscow: ASV Publishing House, 386 p.
- Osokin, A. I., Konyushkov, V. V., Dyakonov, I. P. and Le, V. T. (2019). Evaluation of the bearing capacity of the drilling pile for construction of a skyscraper with a developed underground structure. *Bulletin of Civil Engineers*, 4, pp. 58–67. DOI: 10.23968/1999-5571-2019-16-4-58-67.
- Shashkin, A. G. (2014). *Design of buildings and underground structures in complex geological conditions of Saint Petersburg*. Moscow: Publishing house "Academicheskaya Nauka" — Geomarekting, 352 p.
- Shulyatyev, O. A. (2016). *Bases and foundations of high-rise buildings*. Moscow: ASV Publishing House, 392 p.
- Shulyatyev, O. A., Mozgacheva, O. A., Pospekhov, V. S. (2017). *Development of urban underground spaces*. Moscow: ASV Publishing House, 510 p.
- Ter-Martirosian, A. Z., Ter-Martirosian, Z. G. and Luzin, I. N. (2017). Stress-strain condition of base of deep foundations. *PNRPU Bulletin. Construction and Architecture*, 8 (2), pp. 96–103. DOI: 10.15593/2224-9826/2017.2.09.
- Ter-Martirosyan, Z. G. (2009). *Soil mechanics*. Moscow: ASV Publishing House, 553 p.
- Ter-Martirosyan, A. Z., Ter-Martirosyan, Z. G., Trinh, T. V. and Luzin, I. N. (2015). Sediment and bearing capacity of long pile. *Vestnik MGSU (Monthly Journal on Construction and Architecture)*, 10 (5), pp. 52–61.

СОПРОТИВЛЕНИЕ ПЕСЧАНЫХ И ГЛИНИСТЫХ ГРУНТОВ ПО БОКОВОЙ ПОВЕРХНОСТИ И ПОД ОСТРИЕМ БУРОВЫХ СВАЙ ГЛУБОКОГО ЗАЛОЖЕНИЯ

Владимир Викторович Конюшков¹, Ван Чонг Ле²

^{1,2}Санкт-Петербургский государственный архитектурно-строительный университет
2-ая Красноармейская ул., 4, Санкт-Петербург, Россия

¹E-mail: v.konyushkov@yandex.ru

Аннотация

Санкт-Петербург характеризуется сложными инженерно-геологическими условиями из-за наличия значительной толщи (20...30 м и более) сильнодеформируемых грунтов с модулями общей деформации 5...10 МПа. Кроме этого, вследствие длительных геологических процессов, происходивших на территории Санкт-Петербурга тысячи лет назад эти грунты крайне неравномерно распределены по глубине и площади залегания. Однако современные требования по развитию города требуют более глубоких подземных сооружений и более высоких зданий. Выполнить эти требования с точки зрения геотехнических решений возможно путем применения свай глубокого заложения. **Цель исследования.** Краткая приблизительная классификация геологических условий Санкт-Петербурга по генезису, глубине залегания и ориентировочным физико-механическим свойствам и разработка методики для более точных расчетов несущей способности буровых свай глубокого заложения. **Методы.** В исследовании была применена статистическая обработка 600 значений несущей способности свай, вычисленной по требованиям норм и определенной по результатам полевых испытаний. Кроме этого, была выполнена нелинейная экстраполяция трений и сопротивлений грунтов до глубины 100 м. **Результаты.** В статье представлены результаты исследования: оценка несущей способности буровых свай в зависимости от глубины их расположения в ледниковых моренных и дочетвертичных вендских отложениях. Далее путем нелинейной экстраполяции определены расчетные трения по боковой поверхности и сопротивления под острием буровых свай для проектирования свайных фундаментов из буровых свай глубокого заложения. **Обсуждение.** Фактическая несущая способность буровых свай значительно превышает расчетную, вычисленную по нормам (в 1,6...2,6 раза). На этапе предварительного проектирования фундаментов можно использовать карты глубин залегания кровли ледниковых моренных отложений и дочетвертичных вендских глин и проектировать длину свай исходя из месторасположения объекта строительства в Санкт-Петербурге. Результаты нелинейной экстраполяции сопротивления грунтов сведены в таблицы и графики, применение которых позволит более точно рассчитывать несущую способность буровых свай глубокого заложения.

Ключевые слова

Ледниковые моренные и дочетвертичные вендские отложения, трение грунтов по боковой поверхности свай, сопротивление грунтов под острием свай, несущая способность буровых свай по грунту с длиной до 100м.

Surface Transportation Engineering Technology

IMPROVING THE ACCURACY OF STIFFNESS COEFFICIENT CALCULATION WHEN ESTIMATING THE KINETIC ENERGY SPENT ON VEHICLE DEFORMATION

Stanislav Evtyukov¹, Egor Golov², Jarosław Rajczyk³

^{1,2}Saint Petersburg State University of Architecture and Civil Engineering
Vtoraja Krasnoarmeyskaya st., 4, Saint Petersburg, Russia

³Częstochowa University of Technology
Dabrowskiego st, 69, Czestochowa, Poland

²Corresponding author: egorgoloff@yandex.ru

Abstract

Introduction: The paper addresses a method to estimate the kinetic energy spent on deformations and the vehicle speed equivalent to such value during the reconstruction of road accidents. **Purpose of the study:** The study is aimed at improving coefficients used in the method and affecting the vehicle speed at the instant of a collision. **Methods:** The damage analysis algorithm measures the vehicle deformation to estimate the energy required to produce the measured vehicle damage, with regard to the principle of momentum conservation. **Results:** The stiffness coefficients used were developed long before the appearance of modern vehicles. Therefore, the authors propose to substitute the stiffness coefficients used for those considering modern trends in the automobile industry and ensuring much simpler and more direct calculation. It saves us the trouble to reduce experimental results to the formulation of force deflection and makes it possible to simulate damage behavior directly. The authors also describe the scope of application for the proposed coefficients, and restrictions of their use.

Keywords

Vehicle speed, road accident, road accident reconstruction, kinetic energy, vehicle stiffness, vehicle stiffness coefficients.

Introduction

The existing method for the reconstruction of road accidents (CRASH3) includes two separate and independent algorithms based on:

- 1) analyzing the trajectory of a vehicle involved in the accident (trajectory analysis);
- 2) analyzing vehicle deformations (damage analysis).

Both algorithms assume that the impact is instantaneous and that at some instant of time during the impact both vehicles reach a common velocity. Due to these assumptions, the CRASH3 method cannot be used to reconstruct road accidents involving rollovers, multiple impacts to the same area (superposition of deformations), towing of a trailer or another vehicle (Dobromirov and Evtyukov, 2016).

The trajectory analysis algorithm is based on work–energy relationships for the spinout trajectory and the principle of conservation of linear momentum for the collision. The velocity is estimated using data on the final rest location, skid marks, friction coefficient, and point of impact. Then, momentum equations are used to calculate the impact speed and the difference between the vehicle speeds (Lan, Crawford and Xin, 2006).

In case of impacts, where the line of action of the collision force is not perpendicular to the involved side, the algorithm uses the spinout trajectory and the principle of conservation of linear momentum to calculate the impact speeds and the difference between the vehicle speeds. The damage analysis algorithm is also used for such calculations. The difference between the vehicle

speeds obtained using these two algorithms is rarely the same (Evtuykov and Vasilyev, 2015). However, it can be assumed that the difference between those two estimates is satisfactory when the results differ in not more than 4 km/h or 10% (Evtuykov and Golov, 2019).

Due to the fact that a considerable amount of time passes between the accident and the beginning of the expert examination, and most pieces of evidence, e.g. tire marks (besides, vehicles equipped with an anti-lock braking system (ABS) usually do not leave clearly visible skid marks at the accident site), cannot be recorded, experts rarely use this trajectory analysis algorithm.

Subject, tasks, and methods

During damage analysis, the vehicle deformation is measured to estimate the energy required to produce the vehicle damage, with regard to the theory of momentum conservation.

At first, stiffness coefficient A is determined based on crash test results and using the following equation:

$$A = \frac{m_t \times v_{min} \times b_1}{3.6^2 \times L_t} \tag{1}$$

where:

m_t is the actual vehicle mass before its use in the crash test, kg;

L_t is the width of the measured area of the test vehicle volumetric deformation, m;

v_{min} is the minimum speed of the vehicle hitting a deformable barrier when the volumetric deformation still does not occur, km/h;

b_1 is the share of speed distribution over the contact area, (km/h)/m.

Then, stiffness coefficient B is determined based on crash test results:

$$B = \frac{m_t \times b_1^2}{3.6^2 \times L_t} \tag{2}$$

The share of speed distribution over the contact area is calculated by the following equation:

$$b_1 = \frac{v_t - v_{min}}{C_{AVERT}} \tag{3}$$

where:

v_t is the test vehicle speed at the moment of hitting a deformable barrier (according to NCAP crash test requirements related to a head-on collision with a barrier), $V_t = 35 \text{ mph}$;

C_{AVERT} is the statistically average value of C_i damage depth measurements within the system of six measurement points ($n = 6$), with regard to the test vehicle.

To determine the statistically average value of test vehicle damage depth measurements, the following equation can be used:

$$C_{AVERT} = \frac{\frac{C_1}{2} + \sum_{i=2}^{n-1} C_i + \frac{C_n}{2}}{n - 1} \tag{4}$$

where:

C_i is the depth of the volumetric deformation in the i^{th} point (where $n = 6$), according to the results of measuring the test vehicle damage profile, m (an example of measuring the damage depth is given in Figure 1).

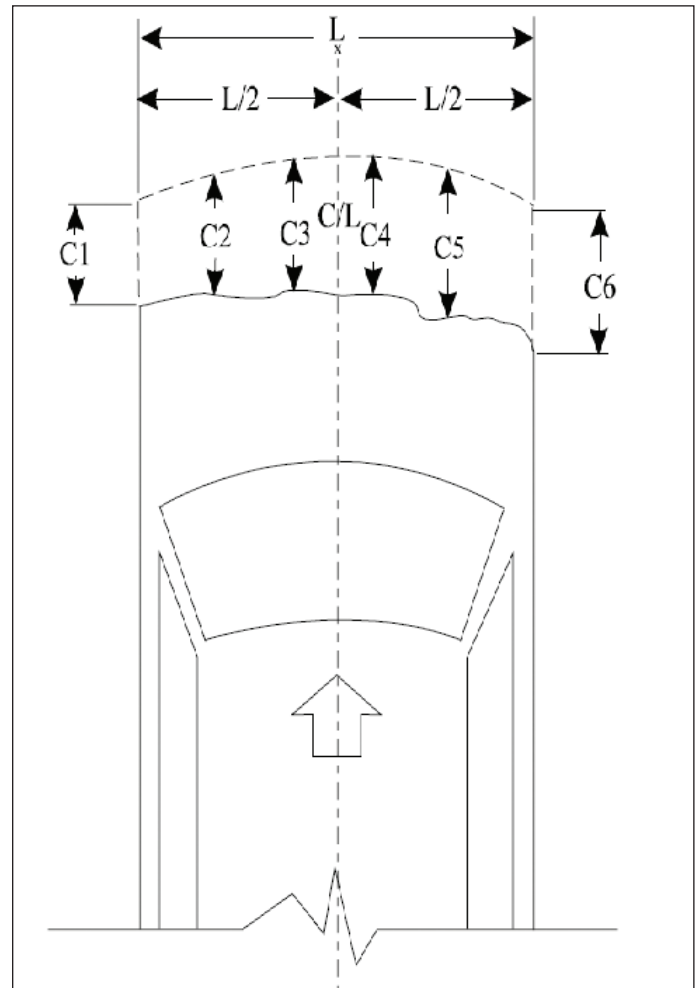


Figure 1. Linear surveying to measure the damage depth and referencing of measurements in case of a head-on collision.

At this stage of selecting coefficients when determining the kinetic energy spent on the vehicle deformation in a road accident, it is required to calculate stiffness coefficients G:

$$G = \frac{A^2}{2 \times B} \tag{5}$$

Then, the length of the measured section in meters is determined:

$$w_i = \frac{L_t}{n - 1} \tag{6}$$

Based on the selected and calculated coefficients, it is possible to determine the work of forces with regard to the deformation and obtain the average deformation volume:

$$E_D = \sum_{i=1}^{n-1} w_i \times \left(\frac{B}{6} \times (C_i^2 + C_i \times C_{i+1} + C_{i+1}^2) + \frac{A}{2} \times (c_{i+1} + c_i) + G \right) \times (1 + \tan^2 \theta) \tag{7}$$

where:

Θ is the angle of the deformation force (along the momentum vector) with account for the results of inspection regarding the vehicle involved in the road accident under consideration, degrees.

The result—the equivalent speed of the vehicle spent on the volumetric deformation—is calculated by the following equation:

$$V_D = 3.6 \sqrt{\frac{2 \times E_D}{m}} \quad (8)$$

where:

m is the vehicle mass with account for the load at the instant of the collision, kg.

The CRASH3 damage analysis algorithm is based on an assumed linear relationship between the impact speed and crush as well as data on crash tests performed with the use of old (1971–1974) four-wheel drive vehicles manufactured by General Motors. Vehicles of later model years have a unified body and significant changes in materials and design. Therefore, it is necessary to refine the coefficients used in the CRASH3 algorithm (National Highway Traffic Safety Administration, 2019). The present paper addresses stiffness coefficients that are either calculated according to the method presented above or selected based on unified values. In particular, we suggest substituting A, B, and G stiffness coefficients used in CRASH3 for β_0 and β_1 . New coefficients ensure much simpler and more direct calculation. It saves us the trouble to reduce experimental results to the formulation of force deflection and makes it possible to simulate damage behavior directly. Stiffness coefficients β_0 и β_1 can be transformed into CRASH3 coefficients A and B as follows:

$$A = \beta_0 \times \beta_1 \quad (9)$$

$$B = \beta_1^2 \quad (10)$$

If β_0 и β_1 stiffness coefficients are used, stiffness parameters of light motor vehicles shall be classified in accordance with the wheelbase and general structural characteristics of a vehicle.

Using the NHTSA’s crashworthiness database, which includes New Car Assessment Program (NCAP) and crash test data, we can assume that the front, side, and rear of a vehicle are characterized by uniform stiffness. Based on NHTSA results, it is proposed to divide vehicles into eight categories corresponding to eight sets of stiffness coefficients (β_0, β_1) (National Highway Traffic Safety Administration, 2019; US Department of Transportation, 1986).

Results

Stiffness coefficients for vehicles can be divided into six categories for light motor vehicles (categories 1–6) according to the wheelbase (see Table 1) and two categories for vans (category 7) and off-roaders (category 8). General stiffness coefficients are given in Table 1.

Table 1. Vehicle stiffness coefficients by categories

Category	Wheelbase, cm	Head-on collision	
		β_0	β_1
1	≤ 240.8	91.4	6.7
2	240.8–258.0	97.0	7.22
3	258.0–280.4	102.1	7.25
4	280.4–298.4	107.0	6.36
5	298.4–312.9	109.6	6.18
6	> 312.9	116.0	5.75
7 (vans)	276.8–330.2	109.7	8.51
8 (off-roaders)	–	105.7	7.98

In case of head-on collisions involving vehicles with a front-wheel drive (FWD), it would be reasonable to have a separate category as larger vehicles usually have a rear-wheel drive and smaller vehicles are more often equipped with an FWD. However, the absence of such a category for FWD vehicles can be explained by the fact that FWD distinctive features are counter-balanced by various wheelbase ranges.

Since the automobile industry is constantly developing, and each model year has different stiffness characteristics, stiffness coefficients shall be updated (refined) at least once a year based on crash tests (Sharma et al., 2007).

Lately, a new vehicle class (sport utility vehicles, SUV) has appeared. The calculated average stiffness coefficients for SUV relatively match the stiffness coefficients for category 7 (vans). However, in the long run, this class would require a separate category.

Since the basic body structure of a particular vehicle model does not change every year, it is possible to use the same stiffness coefficients during those years when no changes are introduced. The stiffness coefficients for vehicles tested can be applied to corresponding “cloned” models (Kirkpatrick et al., 1999).

Discussion

It shall be noted that the stiffness coefficients given have statistically average values with regard to the indicated wheelbase range. It is obvious that the stiffness properties of some vehicles may significantly differ from the data presented.

Besides, β_0 и β_1 coefficients cannot be applied for all types of collisions (e.g. for a collision involving a vehicle with a significantly different clearance).

The algorithm under consideration shall be used in the reconstruction of road and traffic conditions that match crash test conditions as closely as possible. Collisions with displacement, side swipes, and collisions in motion shall be studied more thoroughly. This algorithm may not be

used as a uniform method to estimate accident severity in terms of speed changes (Consolazio et al., 2003).

Conclusions

The authors analyzed the stiffness coefficients used

and proposed to substitute them for those considering modern trends in the automobile industry and ensuring much simpler and more direct calculation. The authors also described the scope of application for the proposed coefficients, and restrictions of their use.

References

- Consolazio, G. R., Chung, J. H. and Gurley, K. R. (2003). Impact simulation and full scale crash testing of a low profile concrete work zone barrier. *Computers and Structures*, 81 (13), pp. 1359–1374. DOI: 10.1016/S0045-7949(03)00058-0.
- Dobromirov, V. N. and Evtyukov, S. S. (2016). “*Scientific rationale for road accident reconstruction based on aerial photographic survey results*” research report. Saint Petersburg: Saint Petersburg State University of Architecture and Civil Engineering, 103 p.
- Dobromirov, V. N., Evtyukov, S. S. and Golov, E. V. (2017). Modern technologies of the primary inspection of the road accident place. *Bulletin of Civil Engineers*, 2, pp. 232–239.
- Evtyukov, S. A. and Vasilyev, Ya. V. (2015). *Guide for expert examination of road accidents*. Saint Petersburg: Petropolis Publishing House, 512 p.
- Evtyukov, S. S. (2014). *Vehicle speed estimation in expert examination of road accidents. PhD Thesis in Engineering*. Saint Petersburg: Saint Petersburg State University of Architecture and Civil Engineering.
- Evtyukov, S. S. and Golov, E. V. (2017). Road traffic safety audit on roads of regional importance in Leningrad region. *Transport of the Urals*, 2, pp. 85–89.
- Evtyukov, S. S. and Golov, E. V. (2019). Selection of coefficients at determining the cost of kinetic energy cost on the vehicle deformation. *Bulletin of Civil Engineers*, 1, pp. 152–157.
- Evtyukov, S. S., Golov, E. V. and Ivanov, N. A. (2019). Innovative safety systems for modern vehicles. *T-Comm*, 13 (6), pp. 71–76.
- Kirkpatrick, S. W., Simons, J. W. and Antoun, T. H. (1999). Development and validation of high fidelity vehicle crash simulation models. In: *IJCrash'98 – International Crashworthiness Conference*. Paper 2000-01-0627. DOI: 10.4271/2000-01-0627. [online] Available at: <https://citeseerx.ist.psu.edu/viewdoc/download?doi=10.1.1.208.5090&rep=rep1&type=pdf> (accessed on: 10.12.2019).
- Lan, S., Crawford, J. E. and Xin, X. (2006). Development of shallow footing anti-ram bollard system through modeling and testing. *Transactions of Tianjin University*, 12(S1), pp. 46–50.
- Medres, E. E., Golov, E. V. and Babenko, T. I. (2017). The factors influencing uniformity of the movement of the motor transport in the conditions of saturated transport streams. *Transportnoye Delo Rossii*, 2, pp. 89–90.
- National Highway Traffic Safety Administration (2019). [online] Available at: www.nhtsa.gov (accessed on: 05.12.2019).
- Sharma, D., Stern, S., Brophy, J. and Choi, E.-H. (2007). An overview of NHTSA's crash reconstruction software WinSMASH. In: *20th International Technical Conference on the Enhanced Safety of Vehicles (ESV)*, June 18–21, 2007. Paper No. 07-0211-W). [online] Available at: https://mafiadoc.com/an-overview-of-nhtsa39s-crash-reconstruction-software-winsmash_59abf8c31723ddbdc5e2b927.html (accessed on: 11.11.2019).
- State Traffic Safety Inspectorate of the Russian Federation (2019). [online] Available at: www.gibdd.ru (accessed on: 15.12.2019).
- US Department of Transportation (1986). CRASH 3 Technical Manual. Cambridge: NHTSA, 458 p.

ПОВЫШЕНИЕ ТОЧНОСТИ ОПРЕДЕЛЕНИЯ КОЭФФИЦИЕНТОВ ЖЕСТКОСТИ ПРИ ОПРЕДЕЛЕНИИ ЗАТРАТ КИНЕТИЧЕСКОЙ ЭНЕРГИИ НА ДЕФОРМАЦИЮ АВТОМОБИЛЯ

Станислав Сергеевич Евтюков¹, Егор Викторович Голов², Jarosław Rajczyk³

^{1,2}Санкт-Петербургский государственный архитектурно-строительный университет
2-ая Красноармейская ул., 4, Санкт-Петербург, Россия

³Ченстоховский политехнический институт
Домбровского ул., 69, Ченстохова, Польша

²E-mail: egorgoloff@yandex.ru

Аннотация

В статье изучается методика определения доли затрат кинетической энергии на развитие деформаций и эквивалентную данным затратам скорость автомобилей при технической реконструкции ДТП. **Цель исследования.** Совершенствование коэффициентов, используемых в методике и влияющих на значение скорости транспортного средства в момент столкновения. **Методы.** Алгоритм анализа повреждений использует измерение деформации ТС для оценки энергии, необходимой для нанесения ТС измеренного ущерба с использованием принципа сохранения импульса. **Результаты.** Используемые коэффициенты жесткости были разработаны задолго до появления современных транспортных средств, в связи с чем предлагается новые коэффициенты жесткости и указывается их область применения. Используемые коэффициенты жесткости, предлагается заменить на новые, концептуально более прямые и простые, а также учитывающие современные тенденции в автомобильной промышленности. Это избавляет от необходимости сводить экспериментальные результаты к формулировке отклонения силы и напрямую моделирует поведение разрушения. Также раскрывается область и ограничения применения предлагаемых к использованию коэффициентов.

Ключевые слова

Скорость транспортного средства, дорожно-транспортное происшествие, реконструкция ДТП, кинетическая энергия, жесткость автомобиля, коэффициенты жесткости автомобиля.

SYSTEMIC INDICATORS OF ROAD INFRASTRUCTURE AT ACCIDENT CLUSTERS

Elena Kurakina¹, Sergei Evtiukov², Grigory Ginzburg³

^{1,2}Saint Petersburg State University of Architecture and Civil Engineering
Vtoraja Krasnoarmeyskaya st., 4, Saint Petersburg, Russia

³International Association of Accident Reconstruction Specialists
United States of America

¹Corresponding author: elvl_86@mail.ru

Abstract

Introduction: To study road infrastructure and ensure control over its changes during its use, it is required to introduce a concept of indicator, which is a parameter or characteristic of road infrastructure facilities' state. Studies on road infrastructure indicators are aimed at traffic safety increase, improvement of a system for road accident forecasting. The authors apply a system for the accounting of road infrastructure facilities' characteristics, set during the design and construction of roads, to forecast road accidents. **Purpose of the study:** The authors develop an approach to studying the influence of systemic indicators of road infrastructure at accident clusters on traffic safety. **Methods:** During the study, such methods as system analysis, extrapolation method, method of forecasting with account for seasonality, and method of repetition were used. **Results:** The authors analyzed statistical data on the road accident rate and identified significant systemic indicators of road infrastructure to assess the efficiency of road and construction measures aimed at traffic safety assurance. They formed groups of indicators in the system of their parametric characteristics and determined conditions of their use to study systemic indicators of road infrastructure. They also determined the capabilities of methods used to forecast the road accident rate to develop an algorithm to analyze road infrastructure at accident clusters. The authors also developed such an algorithm to analyze road infrastructure at accident clusters.

Keywords

Road, indicator, road surface, vehicle, road accident, accident cluster.

Introduction

A system of indicators reflects changes in road infrastructure characteristics set during the design and construction of roads. The system is aimed to detect and prevent violations at various stages of the entire life cycle of a road. Non-compliance with the requirements of technical standards during the design, construction, operation, reconstruction, and maintenance of roads results in the impairment of Driver–Vehicle–Road–Environment (DVRE) system serviceability. In particular, it can lead to the premature destruction of the road surface or formation of defects in it, deterioration in road surface performance affecting its adhesion properties, poor condition of the roadway and shoulders (especially in winter). These factors cause accident-prone situations, decrease traffic safety and increase the number of road accidents. In other words, it is obvious that the Road component of the DRVE system is important in the assurance of traffic safety. It is also confirmed by the start of the “Safe and High-Quality Roads” national project in December 2018

(expected to end in 2024), which includes such plans as Road Network, System-Wide Measures of Road Industry Development, and Traffic Safety. Within the system of traffic safety assurance, various methods are used to solve its functional tasks: forecasting situations in the DVRE system, identifying factors and causes of road accidents, choosing efficient measures intended to increase traffic safety, etc. In this regard, the contribution of the following researchers shall be mentioned: Silyanov V. V. (Moscow Automobile and Road Construction State Technical University (MADI), Moscow); Domke E. R. (Penza State University of Architecture and Civil Engineering, Penza); Brannolte U. (Germany); Pribyl P. (Czech Republic); Kapsky D. V., Kot Ye. N., Vrubel Yu. A. (Belarusian National Technical University, Belarus); St. Petersburg researchers such as Kravchenko P. A., Dobromirov V. N., Evtiukov S. A., Vasiliev Ya. V., Grushetsky S. M., Plotnikov A. M. (Saint Petersburg State University of Architecture and Civil Engineering, Saint Petersburg). They gave

significant attention to studies on the Road component and published numerous papers on the matter that included:

- results of studying the transport and operating conditions of roads, including the determination of a dynamic pattern in braking and adhesion characteristics of vehicle wheels on the road surface at the stage of road operation and reconstruction (Brannolte et al., 2017; Domke and Zhetskova, 2011);

- modeling of the mortality rate as a result of road accidents, considering the road factor and with regard to roads of regional significance (Vrubel et al., 2006);

- results of studies aimed at reducing the number of jams and controlling the capacity of highways with account for the geometry of roads (Domke and Zhetskova, 2011);

- results of studies on transport and pedestrian traffic management. Some researchers laid the groundwork for the use of special traffic lights increasing the efficiency of coordinated traffic management (Evtiukov et al., 2017; Kravchenko, 2013);

- method of road accident reconstruction with account for the technical condition of a vehicle and road environment; results of analyzing accident clusters with the development of efficient traffic safety measures (Kravchenko and Oleshchenko, 2017; Kurakina, 2018; Kurakina et al., 2018; Rajczyk et al., 2018).

The conducted studies were, to an extent, of local nature. Their results do not provide any tools to perform a comprehensive qualitative evaluation with regard to the influence of the road / road infrastructure / road environment state on the appearance and development of prerequisites to the emergence of accident clusters. The analysis of the results provided by the researchers mentioned above confirms that it is necessary to apply an integrated approach to the use of systemic indicators of road infrastructure to determine causes, factors and risk metrics of road accidents, and detect accident clusters. Along with that, it is required to improve methods of road accident forecasting, such as methods of conflict situations and potential dangers, extrapolation, forecasting with account for seasonality, and repetition to prevent or rule out the emergence of accident clusters. Databases on the state of road infrastructure facilities, developed during the design and construction of roads, play an important role in the implementation of these methods.

Due to the evaluation of the actual accident cluster state, it is possible to assess road infrastructure, its safety, and potential accident risk (Evtiukov and Vasiliev, 2008). Based on identified deficiencies and cases of non-compliance with regulatory documents, we can assess the compliance of roads with rules and regulations with account for the relief and climate of the district at the stage of their operation. At the stage of evaluation, the analysis of qualitative and quantitative characteristics of the traffic flow, vehicle braking, and road pavement durability in terms of modulus of elasticity played an important role (Kurakina et al., 2017).

Due to the analysis and processing of data obtained using diagnostic methods, it is possible to determine if the actual state of road infrastructure meets regulatory

requirements. Road infrastructure indicators based on such a study allow us to develop measures aimed at the elimination of black spots, accident rate decrease, increase in the reliability of conclusions and accuracy of calculations when carrying out expert examination following road accident reconstruction (Federal Road Agency (Rosavtodor), 2015; Ilarionov, 1989).

Subject, tasks, and methods

The subject of the study is road infrastructure indicators affecting traffic safety assurance.

The tasks of the study are as follows:

- to assess the possibility of using traditional methods of road accident rate forecasting to develop an algorithm to analyze road infrastructure at accident clusters;

- to analyze statistical data on the road accident rate and provide a rationale for systemic indicators of road infrastructure to assess the efficiency of the proposed road and construction measures aimed at reducing the number of road accidents;

- to form a group of indicators for the system of facilities' parametric characteristics and provide a rationale for the conditions of their use to analyze road infrastructure at accident clusters.

To solve the tasks set, the authors used methods of conflict situations and potential dangers, system analysis, extrapolation, forecasting with account for seasonality, and repetition to prevent or rule out the emergence of accident clusters. They also used software-based computational methods, methods of the probability theory, methods or results' processing, and information technologies.

Results and discussion

To analyze the accident rate, the authors used statistical data on the number of road accidents, including accidents with injuries and fatalities. The results of the analysis (with the Leningrad Region as an example) are given in Figures 1 and 2. They show that up to 25% of all road accidents are caused by the poor condition of roads (including up to 26% with injuries and up to 29% with fatalities).

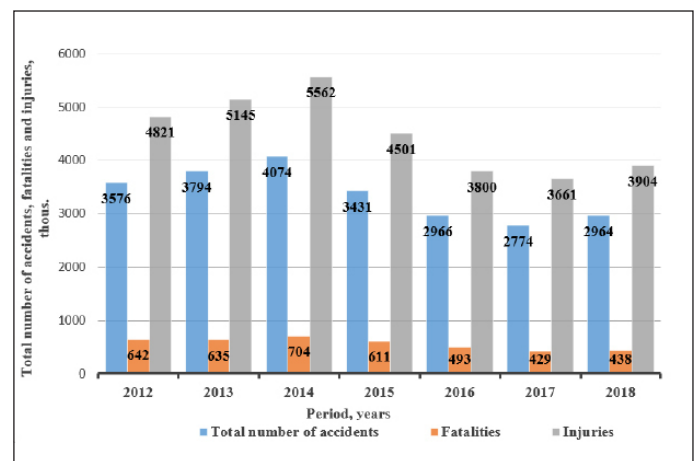


Figure 1. Accident rate on regional public roads in the Leningrad Region during 2012–2018

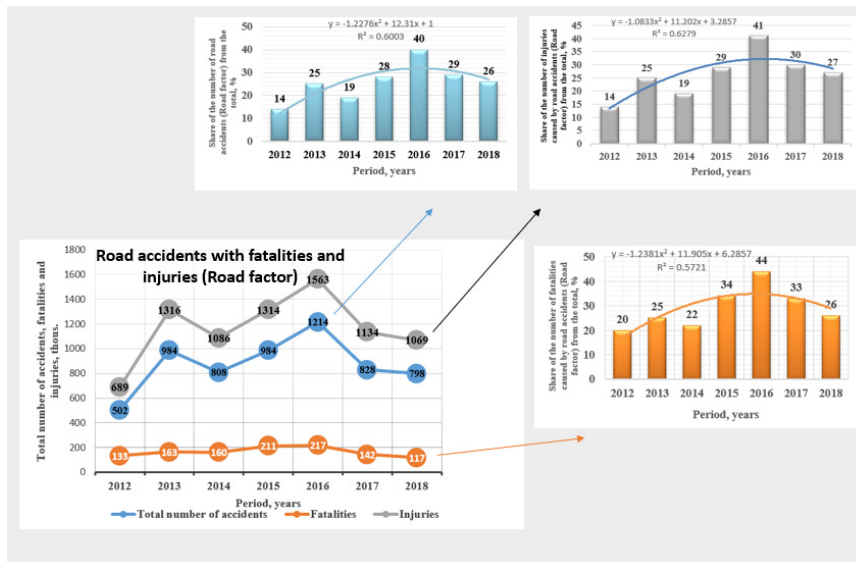


Figure 2. Trend changes in road accidents (with killed and injured persons) due to the poor condition of roads in the Leningrad Region from January 2012 to December 2018, %

The polynomial trend changes in road accidents (with killed and injured persons) regarding the Road factor (Figure 2) allow us to forecast the accident rate on roads. To minimize the contribution of the Road factor in the emergence of road accidents, a system of road infrastructure

indicators is required. By monitoring such indicators, it is possible to forecast prerequisites for road accidents. For that purpose, various analytical methods of assessing traffic safety in road infrastructure can be used (Kapitanov et al., 2018; Plotnikov, 2016; Suvorov et al., 1990).

Table 1. Analytical methods of traffic safety assessment

No.	Method	Characterizing parameters	Studied parameters
1	Safety factor method	Maximum traffic speed at the analyzed road segment — V_{max}^{TF} , vehicle's initial speed — V_{init} .	Traffic intensity. Shoulder-to-shoulder width and width of shoulders. Clear vision distance (plan and profile views). Longitudinal grade. Curve radius in the road cross-section (on long ascending grades)
2	Accident rate factor method	Partial accident rate factors — K_i . The final accident rate — K_{acc} — depends on the number of K_i obtained from the analyzed site	Results of road accident statistical analysis. Traffic intensity. Shoulder-to-shoulder width and width of shoulders. Number of traffic lanes. Clear vision distance (plan and profile views). Longitudinal grade. Clear vision (plan and profile views). Vertical curves (plan view). Grade separation. Road surface condition (Federal Road Agency (Rosavtodor), 2015; Ilarionov, 1989).
3	Black spot identification method	Absolute and relative number of road accidents	Traffic intensity. Results regarding road accidents with injuries.

During traffic safety assessment using analytical methods, only a few parameters are studied, which compromises the quality of evaluating causes of accident clusters' emergence and accident rate forecasting.

In the course of forecasting, it is possible to apply mathematical methods to evaluate changes in the accident rate on roads. It has been established that it is reasonable to apply the extrapolation method only in the case of short-term accident rate forecasting. The method is applied

based on a statistical data array regarding the number of persons killed and injured in road accidents for at least three years. Extrapolation is performed for the subsequent period. When processing extrapolation results, we determine the level of significance indicating the probability of erroneous conclusion. The level of significance (α) may differ for actual and estimated data. Such a situation points to the fact that extrapolation is not suitable for forecasting. The method of forecasting with account for seasonality is

based on an assumption that the number of road accidents depends on the season. When this method is applied, data for at least one year (by months) are used to evaluate the road accident dynamics. However, this method cannot provide a qualitative assessment of the accident rate since the analysis lacks additional data on the state of the road and road environment. The method of repetition is based on the forecasting and changing of one parameter used to analyze statistical data (e.g. the number of road accidents per day). If during the calculation of the level of significance α , actual and estimated values differ, this suggests that the situation analyzed is not described to the fullest extent possible. Therefore, when applying traditional methods of forecasting, it is possible to face the following disadvantages:

- high calculation error;
- inapplicability of some individual results to generate a general forecast;
- insufficient number of indicators, characterizing the state of the road and road environment, taken into consideration (Suvorov et al., 1990).

Therefore, to obtain more accurate forecasting results, it is necessary to account for the significant number of indicators and their parameters that can become a potential cause of a road accident. Currently, the Road factor metrics, characterized by road infrastructure indicators, are the least studied.

In the field of road construction, road operation and reconstruction, it is necessary to take into account the system of parametric characteristics of road facilities

and conditions for their existence: the geometry of road environment facilities (GREF); transport and operating conditions (TrOC); technical and operating conditions (TechOC); the state of road infrastructure facilities (SRIF).

The parametric characteristics of road facilities and conditions were evaluated in the Road – Accident Cluster – Forecast system. Due to the detection and analysis of accident clusters, it became possible to obtain absolute and relative values for the number of road accidents, perform system analysis for each accident cluster. It is suggested to determine GREF, TrOC, TechOC, SRIF values at an accident cluster, using a system of road infrastructure indicators obtained based on parametric data on the passportization of roads, instrumental evaluation and diagnostics of changes in their actual state.

Table 2 suggests road infrastructure indicators for the system analysis of accident clusters.

Due to the analysis of accident clusters using road infrastructure indicators, it is possible to solve the following tasks:

- to evaluate traffic safety on a road operated, as well as the accident rate and its change trends;
- to reduce the number of road accidents and their severity;
- to improve transport and operating characteristics of a road;
- to identify accident clusters;
- to bring infrastructure development elements and traffic management equipment in line with applicable regulations.

Table 2. Road infrastructure indicators for the system analysis of accident clusters

Road infrastructure indicator to be analyzed	Description of the road infrastructure indicator to be analyzed
Geometry of road environment facilities	
N_i	Number of traffic lanes
W_{pull}	Width of the pullover, m
$W_{div.str.}^{centr}$	Width of the central dividing strip, m
W_{marg}^{sh}	Width of the margin strip, m
S_{marg}^{sh}	Width of the margin strip, m (state of the margin strip)
L_{stop}	Width of the stopping lane, m
i	Longitudinal grade, per mille
i_{trans}	Transverse grade, per mille
i_r	Raised curve grade, per mille

Groups of items within the system of parametric characteristics of road facilities and conditions for their existence	R_{curve}	Curve radii in plan, m
	S_{cl}	Clear vision distance to the object, m
	R_{convex}	Radii of convex curves in profile, m
	$R_{concave}$	Radii of concave curves in profile, m
	h_f	Depth of fill, m
	h_e	Depth of excavations, m
	\angle_{slope}	Slope grade
	Transport and operating conditions	
	I_{veh}	Traffic intensity, vehicles/day
	V_{veh}	Allowable vehicle speed, km/h
	G_{veh}	Allowable axial load, t
	K_p^{I-V}	Braking performance coefficient for ground vehicles
	N_{acc}	Number of road accidents
	ACC_{abs}	Absolute accident rate indicator
	ACC_{rel}	Relative accident rate indicator
	C_{veh}	Vehicle categories according to the classification of the UN Eurasian Economic Commission
	Technical and operating conditions	
	ϕ	Road/tire adhesion coefficient
	t	Depth of the road track (wheel tracking), m
	r	Roughness of the road surface, average height of material projection, 10–6 m
	E	Modulus of elasticity of the road surface, MPa
	$D_{r.s.}$	Parameters of road surface defects
	State of road infrastructure facilities	
	$T_{a.s.}$	Artificial structures
	T_{drain}	Drainage systems
	T_{km}^{post}	Kilometer posts
	T_{light}	Lighting
	T_{rail}	Railway crossings
TME	Traffic management equipment	

– to elaborate effective management decisions as well as measures for the elimination of black spots (current and forward-looking measures) and high-priority measures for the prevention of black spot formation (current and forward-looking measures);

– to evaluate changes in the accident rate indicators as a result of implementing measures to improve traffic safety. Figure 3 shows an algorithm of analyzing road infrastructure at accident clusters with the use of the indicators.

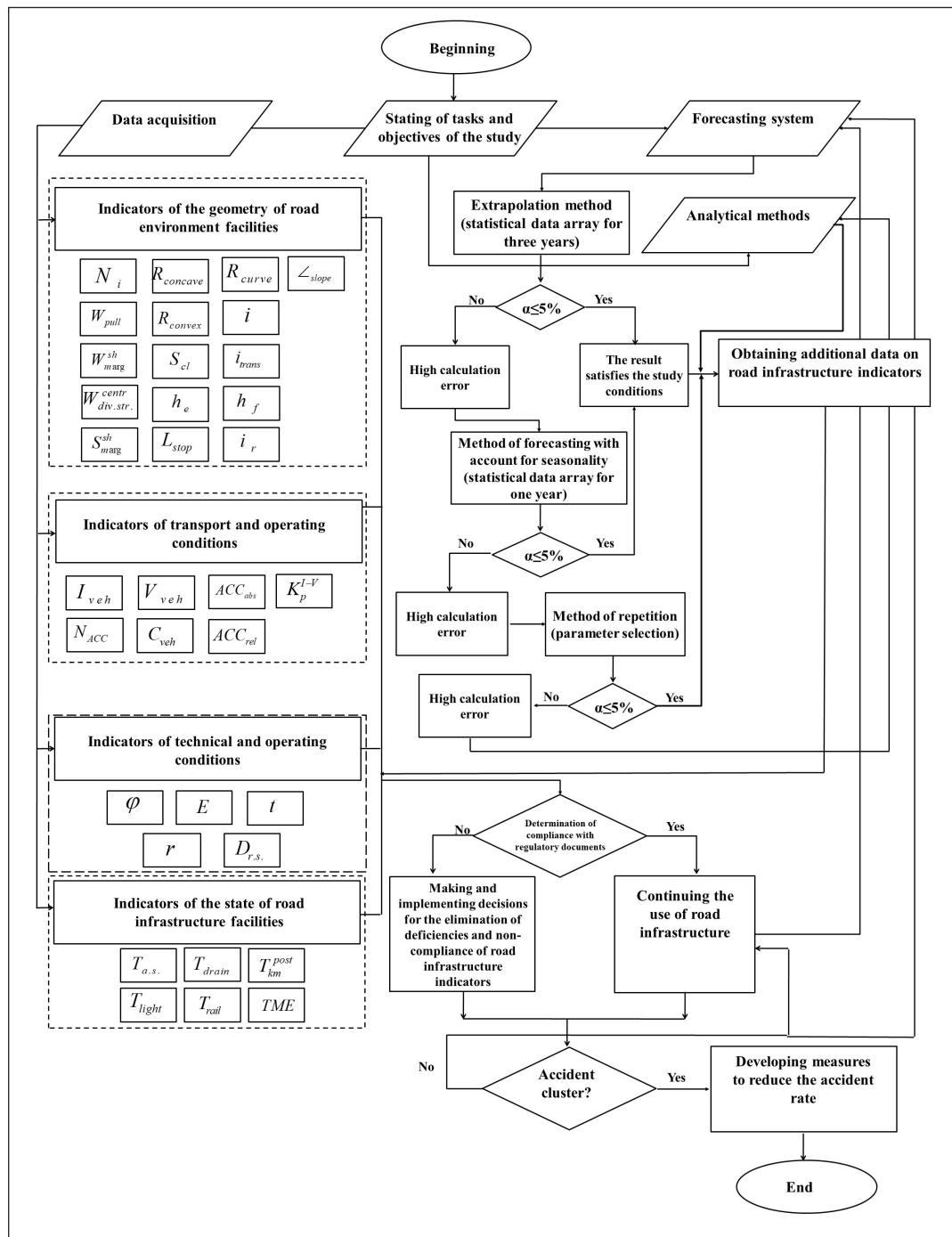


Figure 3. Algorithm of road infrastructure analysis at accident clusters

Conclusions

Based on the analysis of statistical data on the road accident rate, the systemic indicators of road infrastructure were determined. Due to the use of the system of road

infrastructure indicators, it will be possible to ensure traffic safety both at the stage of road design and construction and at the stage of road operation.

References

- Brannolte, U., Silyanov, V., Chubukov, A., Kapitanov, V. and Monina, O. (2017). Simulation of regional mortality rate in road accidents. *Transportation Research Procedia*, Vol. 20, pp. 112–124. DOI: 10.1016/j.trpro.2017.01.031.
- Domke, E. R. and Zhestkova, S. A. (2011). Probabilistic model brakes wheeled vehicles. *The World of Transport and Technological Machinery*, 2, pp. 3–7.
- Evtiukov, S., Kurakina, E., Lukinskiy, V. and Ushakov, A. (2017). Methods of accident reconstruction and investigation given the parameters of vehicle condition and road environment. *Transportation Research Procedia*, Vol. 20, pp. 185-192. DOI: 10.1016/j.trpro.2017.01.049
- Evtiukov, S. A. and Vasiliev, Ya. V. (2008). *Road accidents: investigation, reconstruction, expert examination*. Saint Petersburg: Publishing House DNK, 392 p.
- Federal Road Agency (Rosavtodor) (2015). *Recommendations for accounting and analysis of road accidents on the roads of the Russian Federation. Industrial Road Guidance Document ODM 218.6.015-2015*. Moscow: Federal Road Agency (Rosavtodor), 78 p.
- Ilarionov, V. A. (1989). *Expert examination of road accidents*. Moscow: Transport, 255 p.
- Kapitanov, V., Silyanov, V., Monina, O. and Chubukov, A. (2018). Methods for traffic management efficiency improvement in cities. *Transportation Research Procedia*, Vol. 36, pp. 252–259. DOI: 10.1016/j.trpro.2018.12.077.
- Kravchenko, P. A. (2013). Traffic safety and management in large cities. *Science and Engineering for Roads*, 1, pp. 1–2.
- Kravchenko, P. and Oleshchenko, E. (2017). Mechanisms of functional properties formation of traffic safety systems. *Transportation Research Procedia*, Vol. 20, pp. 367–372. DOI: 10.1016/j.trpro.2017.01.051.
- Kurakina, E. V. (2018). On the effectiveness of studies carried out at places of road traffic accident concentration. *Bulletin of Civil Engineers*, 2, pp. 231–237. DOI: 10.23968/1999-5571-2018-15-2-231-237.
- Kurakina, E. V., Evtiukov, S. S. and Golov, E. V. (2017). *Reconstruction of road accidents*. Saint Petersburg: Petropolis Publishing House, 204 p.
- Kurakina, E., Evtiukov, S. and Rajczyk, J. (2018). Forecasting of road accident in the DVRE system. *Transportation Research Procedia*, Vol. 36, pp. 380–385. DOI: 10.1016/j.trpro.2018.12.111.
- Plotnikov, A. M. (2016). *A method of ensuring traffic safety at controlled intersections in megacity street and road networks. DSc Thesis in Engineering*. Saint Petersburg: Saint Petersburg State University of Architecture and Civil Engineering.
- Rajczyk, P., Kurakina, E. and Knapiński, M. (2018). The influence of surface topography on the safety of road and utility surfaces. *Transportation Research Procedia*, Vol. 36, pp. 640–648. DOI: 10.1016/j.trpro.2018.12.139.
- Suvorov, Yu. B., Kikot, I. M., Khapatnyukovsky, M. V., Kovalenko, L. A. and Kilienko, I. I. (1990). *Diagnostic study of road elements at sections of high accident rate (road conditions) affecting road safety. Guide for experts, investigators and judges*. Moscow: All-Union Research Institute of Forensic Analysis, 93 p.
- Vrubel, Yu. A., Kapsky, D. V., Kot, Ye. N. (2006). *Determination of losses in road traffic*. Minsk: Belarusian National Technical University, 252 p.

СИСТЕМООБРАЗУЮЩИЕ ИНДИКАТОРЫ ДОРОЖНОЙ ИНФРАСТРУКТУРЫ В МЕСТАХ КОНЦЕНТРАЦИИ ДТП

Елена Владимировна Куракина¹, Сергей Аркадьевич Евтюков², Григорий Гинзбург³

^{1,2}Санкт-Петербургский государственный архитектурно-строительный университет
2-ая Красноармейская ул., 4, Санкт-Петербург, Россия

³Вице-президент Международной ассоциации реконструкции и экспертизы ДТП
Соединённые Штаты Америки

¹E-mail: elvl_86@mail.ru

Аннотация

Для исследования дорожной инфраструктуры и контроля за ее изменением в период эксплуатации возникает необходимость введения понятия «индикатор», представляющий собой параметр или характеристику состояния объектов дорожной инфраструктуры. Исследование индикаторов дорожной инфраструктуры направлено на повышение безопасности дорожного движения, совершенствование системы прогнозирования дорожно-транспортных происшествий (ДТП). Реализовано применение системы учета характеристик объектов дорожной инфраструктуры, закладываемых при проектировании и строительстве автомобильных дорог, в интересах прогнозирования ДТП. **Цель исследования.** Разработка подхода к исследованию влияния системообразующих индикаторов дорожной инфраструктуры в местах концентрации ДТП на безопасность дорожного движения. **Методы.** Системный анализ, метод экстраполяции, метод прогнозирования с учетом сезонности, метод повторяемости. **Результаты.** Выполнен анализ статистических данных аварийности на автомобильных дорогах и выявлены значимые системообразующие индикаторы дорожной инфраструктуры с целью оценки эффективности мероприятий дорожно-строительной сферы в обеспечении безопасности дорожного движения (ОБДД). Сформированы группы показателей в системе их параметрических характеристик и определены условия их использования для исследования системообразующих индикаторов дорожной инфраструктуры. Определены возможности методов прогнозирования дорожной аварийности для разработки алгоритма исследования дорожной инфраструктуры в местах концентрации ДТП. Разработан алгоритм исследования дорожной инфраструктуры в местах концентрации ДТП.

Ключевые слова

Автомобильная дорога, индикатор, дорожное покрытие, транспортное средство, дорожно-транспортные происшествия, место концентрации ДТП.